Lisa Kofler, BSc

Characterization of two unknown co-factors of the RNA helicase Prp43 in ribosome biogenesis

MASTER'S THESIS

to achieve the university degree

of Master of Science

Master's degree programme: Molecular Microbiology

submitted to

Graz University of Technology

Supervisor

Priv.-Doz. Dr. Brigitte Pertschy

Institute of Molecular Biosciences

Graz, November 2016

AFFIDAVIT

I declare that I have authored this thesis independently, that I have not used other than the declared sources/resources, and that I have explicitly indicated all material which has been quoted either literally or by content from the sources used. The text document uploaded to TUGRAZonline is identical to the present master‘s thesis.

Date

Signature

Danksagung

An dieser Stelle möchte ich all jenen danken, die mich während meiner Masterarbeit maßgeblich unterstützt haben.

Allen voran möchte ich mich bei Frau Priv. Doz. Dr. Brigitte Pertschy für die ausgezeichnete Betreuung bedanken! Sie hat mich nicht nur fachlich unterstützt, sondern mich immer wieder motiviert und mir mit unglaublicher Geduld meine unzähligen Fragen beantwortet.

Ein großes Dankeschön möchte ich auch meinen Laborkollegen aussprechen, die mir täglich mit Rat und Tat zur Seite standen. Dabei möchte ich mich speziell bei Ingrid bedanken, die mich über die gesamte Zeit vor allem mental sehr unterstützt hat und im Laufe des vergangenen Jahres zu einer wahren Freundin geworden ist.

Ebenfalls möchte ich mich bei meinen langjährigen Studienkolleginnen und Freundinnen Anna und Marlene für die schöne Studienzeit bedanken.

Ein besonderer Dank gilt meinen Eltern, die mich nicht nur im Laufe des Studiums, sondern lebenslang unterstützt und mir immer Rückhalt gegeben haben!

Nicht zuletzt möchte ich mich bei meinem Freund Stephan bedanken, der wahrscheinlich den größten Beitrag am Gelingen dieser Arbeit geleistet hat. Mit unglaublicher Geduld hat er mich immer wieder motiviert und meine Sorgen und Bedenken angehört. Ich weiß, ich war nicht immer einfach! Danke für alles!

Abstract

Characterization of two unknown co-factors of the RNA helicase Prp43 in ribosome biogenesis

Ribosomes function at the heart of every molecular cell life, since they create the proteome. To provide these complex nanomachines, the cell has to face the challenge to coordinate not only the assembly of four ribosomal RNAs and 80 ribosomal proteins, but also the action of not less than 200 ribosomal assembly factors.

One of these factors is the DEAH/RHA helicase Prp43. Initially characterized as mRNA splicing factor, Prp43 was shown to play an essential role in ribosome biogenesis participating in the maturation of both the 40S and the 60S subunit. To regulate its diverse functions co-factors, so called G-patch proteins, are needed. Pxr1 and Pfa1, two yeast G-patch proteins implicated in ribosome biogenesis, were revealed to directly interact with Prp43 and stimulate its otherwise weak ATPase and helicase activities.

Here, we report the characterization of two unknown co-factors of Prp43 implicated in ribosome biogenesis. We identify the uncharacterized Tma23 as novel G-patch protein of Prp43 and show that it directly interacts with the helicase. Furthermore, results from our ATPase assays indicate a potential role of Tma23 as activator of Prp43. Genetic experiments reveal a genetic link between Tma23 and Pxr1, but not with Pfa1.

Additionally, we identified another Prp43 co-factor. Gaf1 (Ycr016w) and Prp43 form a stable complex suggesting a possible function of Gaf1 as Prp43 adapter protein.

Zusammenfassung

Charakterisierung zweier unbekannter Cofaktoren der RNA Helikase Prp43 in der Ribosomenbiogenese

Ribosomen haben zentrale Funktion im molekularen Zellstoffwechsel, da sie durch die Translation das gesamte Proteom der Zelle bereitstellen. Die Synthese dieser komplexen Nanomaschinen stellt eine enorme Herausforderung dar. Nicht nur die Assemblierung der vier ribosomalen RNAs und 80 ribosomalen Proteine muss koordiniert werden, sondern auch die Zusammenarbeit von über 200 Assemblierungsfaktoren.

Einer dieser Faktoren ist die DEAH/RHA Helikase Prp43. Zuerst als mRNA Splicingfaktor charakterisiert, wurde Prp43 auch als essentieller Ribosomenbiogenesefaktor beschrieben, der sowohl an der 40S- als auch an der 60S-Reifung beteiligt ist. Für die Regulation seiner diversen Funktionen sind Cofaktoren, sogenannte G-patch Proteine verantwortlich. Pxr1 und Pfa1, zwei G-patch Proteine der Hefe, interagieren mit Prp43 direkt und stimulieren seine sonst schwachen ATPase- und Helikaseaktivitäten.

Diese Arbeit beschreibt die Charakterisierung von zwei unbekannten Cofaktoren von Prp43 in der Ribosomenbiogenese. Tma23 wird als neues G-patch Protein von Prp43 identifiziert und es wird gezeigt, dass es mit der Helikase direkt interagiert. Außerdem weisen Ergebnisse von ATPase-Assays auf eine Stimulation der Helikase durch Tma23 hin. Auf genetischer Ebene zeigt Tma23 eine Interaktion mit Pxr1, aber nicht mit Pfa1.

Zusätzlich wird ein weiterer Prp43 Cofaktor identifiziert. Gaf1 (Ycr016w) bildet mit Prp43 einen stabilen Komplex, was auf eine mögliche Funktion als Adapterprotein hindeutet.

Content

1 Introduction

1.1 Eukaryotic ribosome biogenesis – an overview

Ribosomes provide cells with their total proteome by translating the genetic information encoded within the mRNA into protein sequences. These highly conserved complex nanomachines consist of two subunits, the small 40S and the large 60S ribosomal subunit. The small subunit comprises the 18S ribosomal RNA (rRNA) and 33 ribosomal proteins and contains the decoding site, where aminoacyl-tRNAs bind the mRNA. The large subunit consists in addition to the three rRNAs (5S, 5.8S and 25S rRNA) of 46 ribosomal proteins and catalyzes the peptide bond formation by its peptidyltransferase activity (Cruz et al., 2015; Woolford and Baserga, 2013).

Especially in rapidly dividing cells the need of ribosomes is tremendous. *Saccharomyces cerevisiae*, for example, synthesizes 2000 ribosomes every minute and thereby doubles its entire set of ribosomes in 1.5 hours (Warner, 1999). During this process, strikingly, not only the assembly of 79 ribosomal proteins and four rRNAs have to be spatially and temporally coordinated, but also the action of all three RNA polymerases and not less than 200 non-ribosomal assembly factors that transiently associate with maturing ribosomal precursors (Kressler et al., 2010; Thomson et al., 2013). It is therefore not surprising that ribosome biogenesis is not only a very energy-consuming, but also enormously intricate process that has to be tightly regulated. In the past, genetic and biochemical experiments in the model organism *S. cerevisiae* provided a good understanding of basic principles of ribosome biogenesis in eukaryotes.

The starting point of ribosome maturation is the nucleolus, a subcompartment of the nucleus, where the RNA polymerase I synthesizes the 35S pre-rRNA, the common precursor of the 18S, 5.8S and 25S rRNAs, that are flanked and separated by external and internal spacers (figure 1). The fourth rRNA (5S rRNA) is transcribed separately by the RNA polymerase III (Henras et al., 2015; Woolford and Baserga, 2013) (figure 1a). Concomitantly, ribosomal proteins and accessory factors, which are both synthesized in the cytoplasm and have to be transported into the nucleus, already assemble with the nascent 35S pre-RNA and form the 90S particle. Upon co-transcriptional exo- and endonuclease activities the 35S pre-rRNA gets processed and cleavage at site A_2, located within the internal spacer 1, separates the 18S precursor rRNA (20S rRNA) from the common precursor of the 5.8S and 25S rRNA ($27SA_2$ rRNA), which splits the maturation pathway of the 40S and the 60S subunit

a

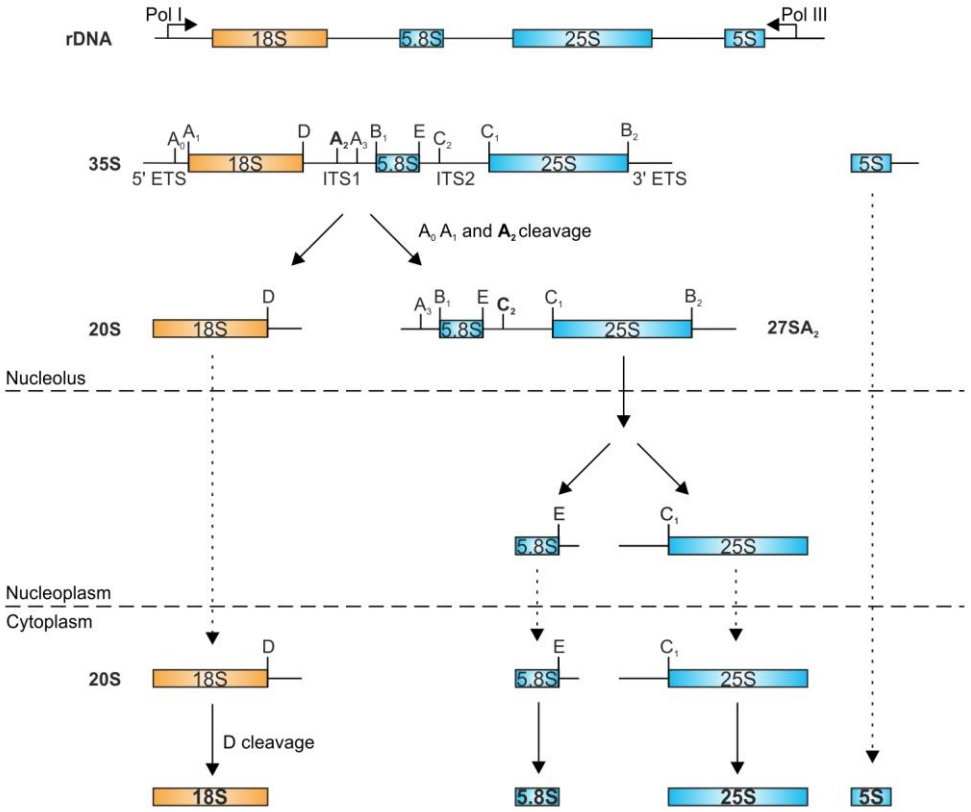

b

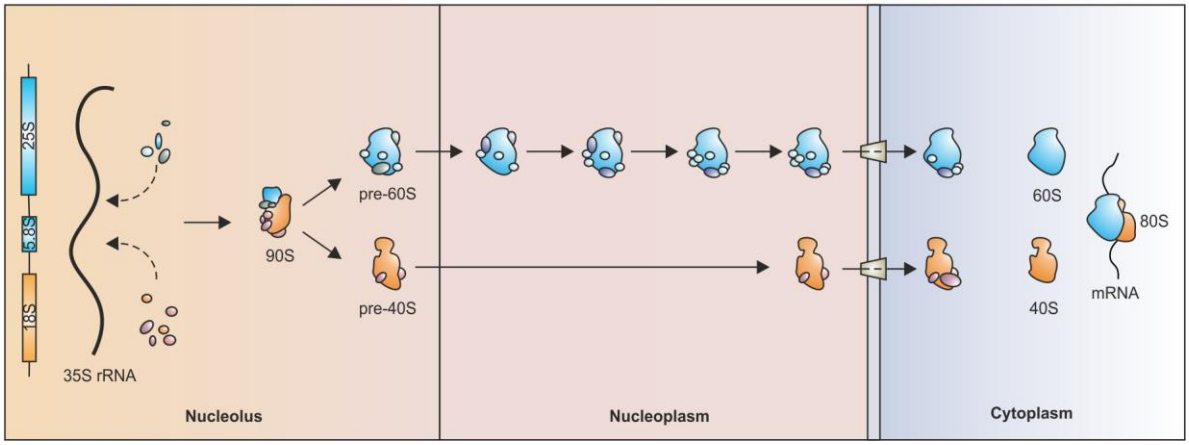

Figure 1: Overview of ribosome biogenesis in eukaryotes. Components of the 40S subunit are indicated in orange, those of the 60S subunit in blue. **(a)** Simplified overview of rRNA processing steps. The RNA polymerase I (Pol I) transcribes the 18S, 5.8S and 25S ribosomal RNAs (rRNAs) as polycistronic 35S precursor rRNA, while the 5S rRNA is transcribed separately by the Polymerase III (Pol III). On the way from the nucleolus to the cytoplasm exo- and endonucleases remove the external and internal spacers (ETS, ITS) and convert the pre-rRNAs into the mature 18S, 5.8.S, 25S and 5S rRNAs. Cleavage sites are indicated. **(b)** Simplified schematic depiction of ribosome biogenesis in eukaryotes. In the nucleolus three of the rRNAs were transcribed as common polycistronic transcript. Upon co-transcriptional protein assembly the 90S particle gets formed. Rearrangements and processing steps follow before the maturation pathway of the pre-40S and the pre-60S particles are separated. While the pre-40S particle is rapidly exported into the cytoplasm, the pre-60S undergoes far more maturation steps prior to its nuclear export across the nuclear pore complex. In the cytoplasm the last maturation steps occur, the subunits join on mRNA and are ready for translation.

(Cruz et al., 2015; Fromont-Racine et al., 2003; Henras et al., 2015; Kressler et al., 2010; Thomson et al., 2013). While the small subunit is almost directly exported to the cytoplasm, where the D-cleavage takes place and the mature 18S rRNA arises, the large subunit undergoes far more rearrangements and rRNA processing steps prior to the export across the nuclear pore complex. In the cytoplasm maturation gets completed by final rRNA processing and dissociation of the last accessory factors. Finally, a proofreading system tests the mature subunits, before they are competent to start their first round of translation (Cruz et al., 2015; Fromont-Racine et al., 2003; Kressler et al., 2010; Thomson et al., 2013; Woolford and Baserga, 2013).

1.2 Ribosomal assembly factors

With the help of genetic and biochemical approaches (including tandem affinity purification (TAP) (Puig et al., 2001) and sensitive mass-spectrometry techniques) mostly performed in *S. cerevisiae* many of the 200 non-ribosomal factors implicated in ribosome biogenesis could be characterized in recent years (Fromont-Racine et al., 2003; Tschochner and Hurt, 2003; Henras et al., 2008). Apart from endo- and exonucleases that are involved in rRNA processing, a couple of assembly factors are required to prevent aggregation and miss folding of the basic ribosomal proteins before they get incorporated into the maturing ribosomal particles. Others act as shuttling factors and transport the export competent pre-ribosomal subunits through the nuclear pore complexes to the cytoplasm. Some assembly factors are energy consuming enzymes like GTPases, AAA-ATPases, kinases and helicases (Cruz et al., 2015; Fromont-Racine et al., 2003; Kressler et al., 2010; Thomson et al., 2013; Woolford and Baserga, 2013) (figure 2). RNA-helicases represent the largest group, comprising up to 20 proteins that are implicated in RNA structural rearrangements, release of snoRNAs, remodeling of rRNA-protein complexes and rRNA processing (Bleichert and Baserga, 2007; Lebaron et al., 2005, 2009).

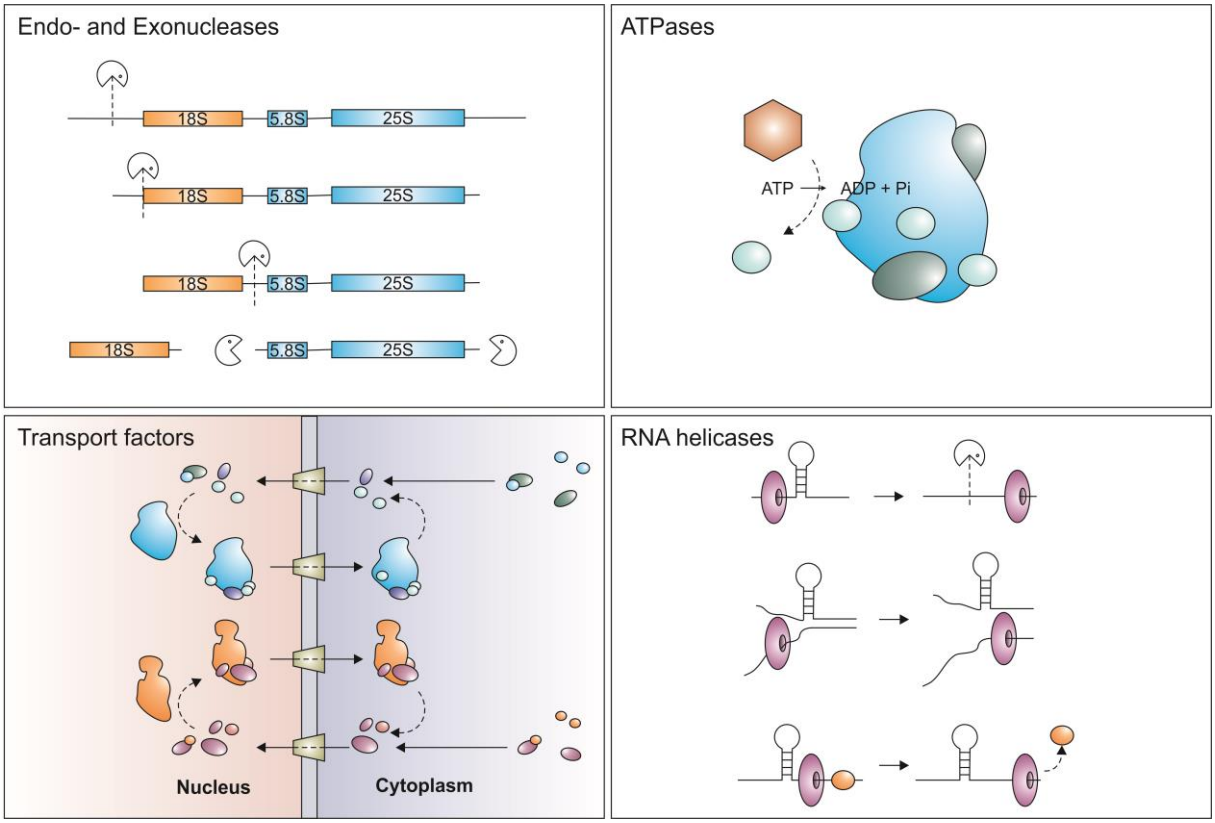

Figure 2: Overview of the function of some assembly factors involved in ribosome biogenesis.

1.2.1 The DEAD/RHA helicase Prp43

RNA helicases are highly conserved enzymes that are involved in nearly all processes of RNA metabolism. According to their conserved motifs RNA helicases can be classified into five superfamilies (SF1 – SF5) (Bleichert and Baserga, 2007; Fairman-Williams et al., 2010; Martin et al., 2013; Nickels and Hochschild, 2004), whereby all RNA helicases found in eukaryotes belong to SF1 or SF2 (Jankowsky, 2011). These helicases contain a characteristic helical core, comprising two tandem RecA-like domains that encompass the NTP hydrolysis, the nucleic acid binding and the helicase activities (Fairman-Williams et al., 2010; Robert-Paganin et al., 2015). One important group within SF2 is the DEAH/RHA helicase family that is named according to the sequence of the Walker B motif (Asp-Glu-Ala-His) and the RNA helicase A, a member of this family. In yeast *S. cerevisiae* seven proteins belong to the DEAH/RHA family: Prp2, Prp16 and Prp22 (DHX16, DHX38 and DHX8 in human) that are involved in mRNA splicing, the ribosome assembly factors Dhr1 (DHX37) and Dhr2 (DHX32) and the uncharacterized, non-essential Ylr419w (DHX29). The seventh member, the bifunctional helicase Prp43 (DHX15) is the most striking one, since it is required

for both mRNA splicing and ribosome biogenesis (Bleichert and Baserga, 2007; Robert-Paganin et al., 2015).

Prp43 (pre-mRNA processing factor) was initially identified as splicing factor required for the disassembly of the lariat-spliceosome complex (Arenas and Abelson, 1997). Since a large scale analysis detected the steady-state localization of Prp43 in the nucleolus (Huh et al., 2003), the speculation came up that it is also implicated in ribosome biogenesis (Lebaron et al., 2005). Indeed, soon after, Prp43 was found in almost all ribosomal precursors from 90S to pre-40S and pre-60S particles. Furthermore, accumulation of 35S pre-rRNA accompanied with a severe reduction of all downstream pre-rRNA processing intermediates upon Prp43 depletion indicated that Prp43 belongs to the few accessory factors that are required for the synthesis of both the 40S and the 60S subunit (Lebaron et al., 2005). Crosslinking and cDNA analysis (CRAC) determined a couple of distinct binding sites on rRNA precursors and corroborated results from genetic experiments that assigned Prp43 to the regulation of 20S rRNA processing by the endonuclease Nob1 (Combs et al., 2006; Leeds et al., 2006; Pertschy et al., 2009; Bohnsack et al., 2009). Additionally, Prp43 and its ATP dependent helicase activity also appeared to be required for the release of snoRNAs during ribosome biogenesis (Bohnsack et al., 2009; Leeds et al., 2006), similar to its recycling function in mRNA splicing. To fulfill its multiple distinct functions during two main cellular processes, Prp43 was shown to be regulated by different co-factors, the G-patch proteins.

1.3 G-patch proteins – the regulators of DEAH/RHA helicases

Despite their otherwise dissimilar protein sequence G-patch proteins harbor a characteristic glycine-rich motif, the G-patch domain that was identified using sequence alignment. The motif comprises up to 50 amino acids and contains the consensus *hhxxx*G*axx*G*xxxx*G, where *h* represents a hydrophobic, *a* an aromatic and *x* a non-conserved residue. According to this study G-patch proteins are highly conserved among eukaryotes but are not present in archaea or bacteria (Aravind and Koonin, 1999). G-patch domains were found in proteins that contain RNA binding domains as well as in regulators of DEAH/RHA helicases. The latter use their G-patch domain to specifically interact with their helicase partner, whereby the oligonucleotide/oligosaccharide (OB)-fold, a particular structural feature of DEAH/RHA helicases was described to be critical for this interaction. Moreover, the G-patch domain was demonstrated to stimulate the ATPase and helicase activity of the DEAH/RHA helicases (Robert-Paganin et al., 2015).

Up to now, five G-patch proteins were identified in *S. cerevisiae*: Spp2, Ntr1/Spp382, Pfa1/Sqs1, Pxr1/Gno1 as well as the poorly characterized Cmg1. While Spp2 is linked to the function of the RNA helicase Prp2 in mRNA splicing, all other four G-patch proteins were described as co-factors of Prp43. Ntr1 regulates the helicase in mRNA splicing, whereas Pfa1 and Pxr1 are required for ribosome biogenesis. For Cmg1 no cellular pathway has been identified so far. Recently, it was reported that the G-patch of these proteins compete for the binding of Prp43 and thus, regulate the distribution of the multifunctional helicase in the different pathways (Heininger et al., 2016).

1.3.1 G-patch protein partners of Prp43

Ntr1 (nineteen complex related protein) was shown to regulate Prp43 during mRNA splicing. Ntr1 and its protein partner Ntr2, both essential for cellular growth, form a stable complex, which further binds the helicase Prp43 via the G-patch domain of Ntr1 (Boon et al., 2006; Tsai et al., 2005). This complex, also called NTR-complex then assembles with the U5 snRNP of the spliceosome, whereby Ntr2 acts as adapter protein that binds directly to U5. However, the Ntr1-Ntr2 complex also associates with the spliceosome independently from Prp43. Thus, the interaction between Ntr1-Ntr2, Prp43 and U5 is a dynamic process. Prp43 can assemble as NTR-complex to the spliceosome or can be recruited by the Ntr1-Ntr2 complex that is able to interact with the spliceosome in a Prp43 independent manner (Tsai et al., 2007) (figure 3). Thereby the interaction between Prp43 and the G-patch domain of Ntr1 was shown to be crucial for the stimulation of Prp43's helicase activity, which is the trigger for the disassembly of the intron-lariat-spliceosome (ILS) complex (Tanaka et al., 2007). Ntr2 and the C-terminal part of Ntr1 were described to function as "doorkeepers" to prevent disassembly of properly working spliceosomes (Fourmann et al., 2016).

Tandem affinity purification and a genome-wide double-hybrid screen identified **Pxr1** (PinX1-related gene) as another co-factor of Prp43 containing a G-patch domain (13). Since it is localized in the nucleolus it is also termed *G-patch nucleolar protein*, Gno1. Strains lacking Pxr1 exhibit a severe growth defect due to an impairment of the first processing steps of the 35S rRNA at sites A_0, A_1 and A_2 (Guglielmi and Werner, 2002). Pxr1-G-patch mutants completely fail to correct the processing defects in *Δpxr1* strains suggesting that the interaction with Prp43 and its stimulation via the G-patch domain are essential for ribosome biogenesis (Chen et al., 2014). Furthermore, it was recently discovered that Pxr1 recruits the helicase to the 90S particle, similar to the function of Ntr1 in mRNA splicing (Unterweger S., in progress).

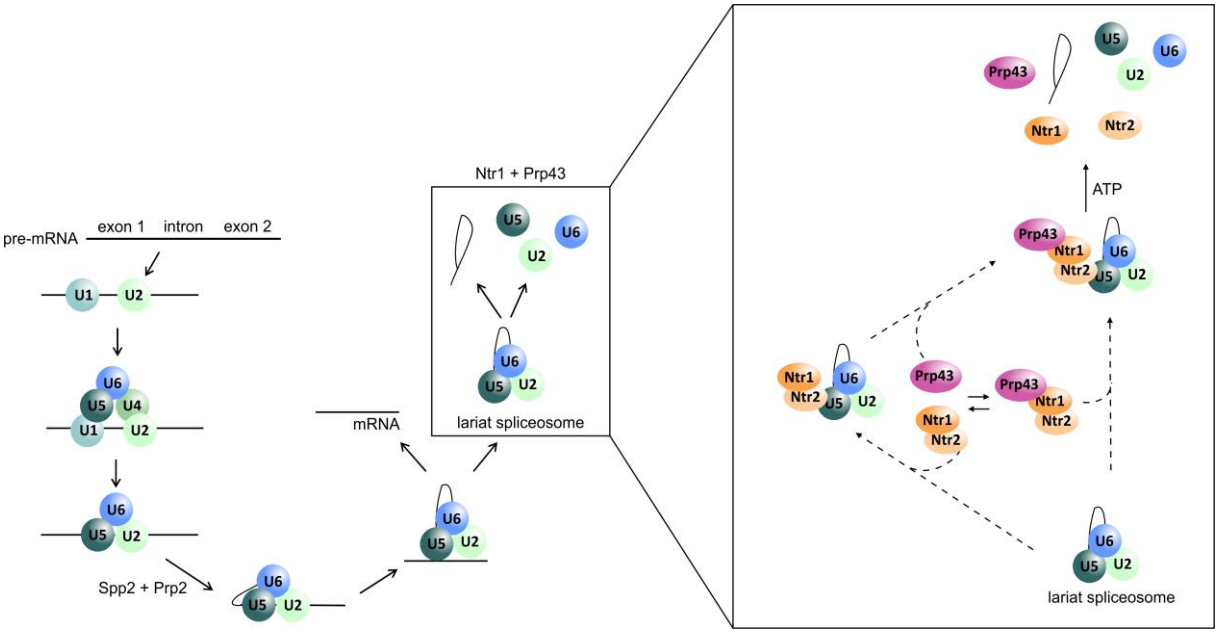

Figure 3: Schematic depiction of mRNA splicing to show the function of G-patch proteins Spp2 and Ntr1. While Spp2 is linked to the function of Prp2 in the first catalytic reaction of mRNA splicing, Ntr1 together with its co-factor Ntr2 contribute to disassembly of the intron-lariat-spliceosome by Prp43. Prp43 can bind to the spliceosome as NTR-complex (Ntr2-Ntr1-Prp43) or can be recruited by Ntr1-Ntr2 that can associate to the spliceosome in a Prp43 independent manner. Ntr2 acts as adapter protein and interacts with U5. (adapted from (Robert-Paganin et al., 2015) and (Tsai et al., 2007))

Pfa1 (Prp fortythree associated) is the most abundant factor that can be found among the proteins co-purified with Prp43 after tandem affinity purification (Lebaron et al., 2005). Interestingly, it was shown that Pfa1 contains two distinct domains that directly interact with Prp43. Beside the C-terminal G-patch containing domain also the N-terminus (amino acids 1-202) harbors the ability to independently bind Prp43 (Lebaron et al., 2009). A synthetic lethal screen exhibited a genetic link between Pfa1, the pre-40S factor Ltv1, the endonuclease Nob1 and Prp43. A severe accumulation of 20S pre-rRNA upon expression of Prp43 mutants or deletion of *PFA1,* when combined with the *LTV1* deletion indicated the contribution of these factors to the processing of 20S to 18S rRNA. Indeed, it was shown that Ltv1, Pfa1 and Prp43 act in a functional network to enable 20S rRNA processing by the endonuclease Nob1 (Pertschy et al., 2009). Only the expression of Pfa1 truncations able to stimulate the helicase activity of Prp43 restore normal 20S and 18S rRNA levels in *Δpfa1* strains depleted for Ltv1 suggesting that stimulation of Prp43's ATPase and helicase activity is required for D-cleavage (Lebaron et al., 2009). Additionally, it was recently shown that Pfa1 has also recruiting functions. However, while Pxr1 is required for the recruitment of Prp43 to very early particles, Pfa1 is capable to stabilize Prp43 on later 90S, pre-40S and pre-60S particles (Unterweger S., in progress).

The fifth G-patch protein known in yeast remained uncharacterized for a long time. Very recently, pull-down experiments using TAP-tagged **Cmg1** identified Prp43 as the helicase interaction partner of Cmg1. It directly interacts with Prp43 via the G-patch domain and stimulates Prp43's ATPase activity. Localization analysis revealed that Cmg1 is located within the cytoplasm and, interestingly, within mitochondria, hence the name *cytoplasmic and mitochondrial G-patch protein 1* (Cmg1). Deletion of Cmg1 does not affect rRNA processing suggesting that its cytoplasmic function is not linked to ribosome biogenesis (Heininger et al., 2016).

1.4 Tma23 and Gaf1 – two uncharacterized proteins as putative Prp43 co-factors

Tma23 (translation machinery associated) is an up to now uncharacterized protein that contains a glycine-rich motif and is linked to ribosome biogenesis (Buchhaupt et al., 2007; Peng et al., 2003) (figure 4). Recently, Prp43 could be co-purified with Tma23-TAP indicating a role of Tma23 as another G-patch protein of Prp43 during ribosome maturation (Unterweger S., in progress). However, to date, the possible function of Tma23 in ribosome biogenesis and its interaction partners are uncharacterized.

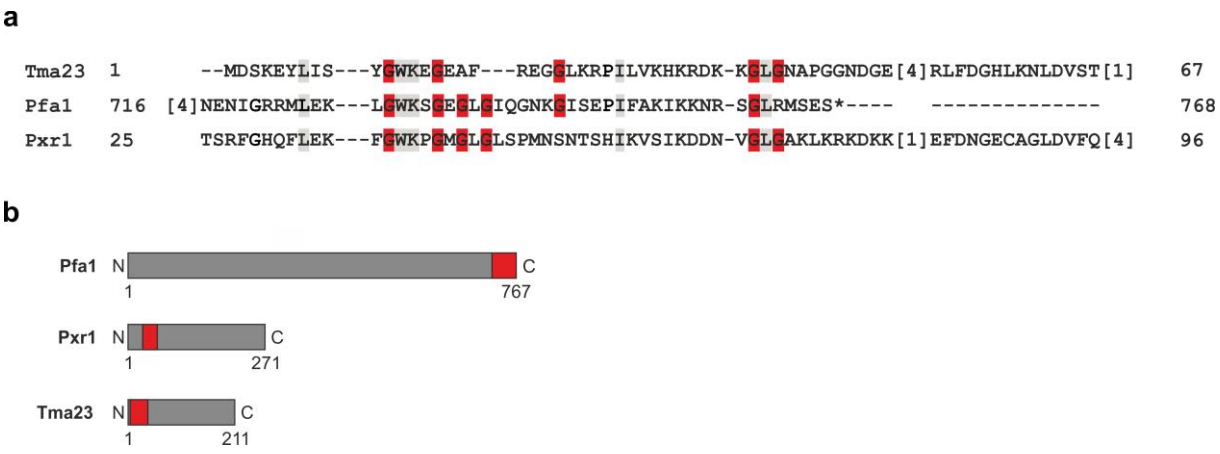

Figure 4: G-patch domains of Pfa1, Pxr1 and Tma23. (a) Sequence alignment of Pfa1, Pxr1 and Tma23. Tma23 also contains a G-patch domain. The numbers refer to the position of the G-patch within each protein. Sequence identities are shaded. (Adapted from Unterweger S., in progress) **(b)** Schematic depiction of Pfa1, Pxr1 and Tma23 with their G-patch domain depicted in red.

Additionally, a protein with unknown function was recently identified in TAPs of three G-patch proteins of Prp43. Pfa1-TAP, Pxr1-TAP as well as Cmg1-TAP co-purify the unknown protein Gaf1/Ycr016w (G-patch protein associated factor 1) (Unterweger S., in progress). TAP of Gaf1 co-purified the helicase Prp43 and many other ribosomal biogenesis factors as interaction partners suggesting that Gaf1 is linked to the function of Prp43 in ribosome

biogenesis. Quite in line with this, Gaf1 was found among proteins co-purified with Prp43-TAP (Lebaron et al., 2005). Together these findings indicate a functional network between G-patch proteins of Prp43, the helicase Prp43 and Gaf1 and raise the hypothesis that Gaf1 acts as adapter protein of Prp43 in ribosome biogenesis, similar to Ntr2 in mRNA splicing.

1.5 Aims of this study

This work focuses on the characterization of the two unknown proteins Tma23 and Gaf1 involved in ribosome biogenesis.

No interaction partner of the G-patch protein Tma23 had been identified so far and nothing was known about its function. To investigate, whether Tma23 represents the third G-patch protein of Prp43 involved in ribosome biogenesis we examined the direct interaction between Tma23 and Prp43 and whether Tma23 is capable to stimulate Prp43's ATPase activity. Additionally, we wanted to check the genetic network between *PFA1, PXR1* and *TMA23* to investigate a redundant role of these proteins in ribosome biogenesis.

Furthermore, we wanted to assess the direct interaction between Prp43 and the uncharacterized Gaf1 to explore a putative role of Gaf1 as adapter protein of Prp43.

2 Materials and Methods

2.1 Strains, plasmids and primers

Saccharomyces cerevisiae strains used in this study are depicted in table 1.

Table 1: *Saccharomyces cerevisiae* strains used in this study.

No.	Name	Genotype	Origin
4018	W303 5C	*MATα ade2 his3 leu2 trp1 ura3 can1-100*	Brigitte Pertschy
4022	Δ*pfa1*	*MATα* Δ*pfa1::hisMX*	Brigitte Pertschy
4020	Δ*tma23*	*MATα* Δ*tma23::trpMX*	Brigitte Pertschy
4026	Δ*pxr1*	*MATα* Δ*pxr1::hphNT1*	Brigitte Pertschy
4035	Δ*pfa1*Δ*pxr1*	*MATα* Δ*pfa1::hisMX* Δ*pxr1::hphNT1*	Brigitte Pertschy
4029	Δ*pfa1*Δ*tma23*	*MATα* Δ*pfa1::hisMX* Δ*tma23::trpMX*	Brigitte Pertschy
4032	Δ*pxr1*Δ*tma23*	*MATα* Δ*pxr1::hphNT1* Δ*tma23::trpMX*	Brigitte Pertschy
4038	Δ*pfa1*Δ*pxr1*Δ*tma23*	*MATα* Δ*pfa1::hisMX* Δ*pxr1::hphNT1* Δ*tma23::trpMX*	Brigitte Pertschy

Plasmids used in this study were constructed using standard recombinant DNA techniques and are listed in table 2, the used primers are depicted in table 3.

The *E. coli* expression plasmid pETDuet-FLAG-*PRP43* was obtained by inserting the Nde1/Xho1-digested *FLAG-PRP43* PCR product that was amplified using the primers Prp43_Nde1_Flag_Fw and Prp43_Xho1_Rev and chromosomal yeast (W303) DNA as template, into the Nde1/Xho1-digested pETDuet-1.

For construction of *E. coli* expression plasmid pETDuet-*YCR016w*-FLAG-*PRP43* the PCR product *FLAG-PRP43* that was amplified using the primers Prp43_Nde1_Flag_Fw and Prp43_Xho1_Rev and chromosomal yeast (W303) DNA as template was digested with Nde1 and Xho1 and was inserted into pETDuet-*YCR016w* digested with the same restriction enzymes.

The *E. coli* expression plasmid pETDuet-*PFA1* was constructed by inserting the BamH1/Sal1-digested *PFA1* PCR product that was amplified using the primers Pfa1_BamH1_Fw and Pfa1_Sal1_Rev and chromosomal yeast (W303) DNA as template, into the BamH1/Sal1-digested pETDuet-1.

Tma23 was codon optimized for expression in *E. coli* by MWG Eurofins.

The *E. coli* expression plasmid pGEX-6P-*TMA23(FL)* was generated by inserting the *TMA23-codon-optimized* PCR product that was obtained using the primers Tma23_synth_BamH1_Fw and Tma23_synth_Sal1_rev and the synthesized *TMA23* fragment (MWG Eurofins) as template after BamH1/Sal1 digestion into the BamH1/Sal1-digested pGEX-6P-1.

The *E. coli* expression plasmid pGEX-6P-*TMA23(1-61)* was obtained by inserting the BamH1/Sal1-digested *TMA23(1-61)-codon-optimized* PCR product that was amplified using the primers Tma23_synth_BamH1_Fw and Tma23opt_aa61_Sal1rev and the plasmid pGEX-6P-*TMA23(FL)* as template, into the BamH1/Sal1-digested pGEX-6P-1. The same template and same restriction enzymes were used to insert the PCR product obtained with the primers Tma23opt_aa62_BamH1Fw and Tma23opt_Sal1_rev into the BamH1/Sal1-digested pGEX-6P-1 for the generation of the expression plasmid pGEX-6P-*TMA23(62-211).*

Table 2: Plasmids used in this study.

No.	Plasmid	Features	Origin
#45	pETDuet-1	Amp^R, co-expression vector for *E. coli,* contains His-tag in front of the MCS1	Novagen
#727	pETDuet- His6-*YCR016w*	Amp^R *,* His6-tag fusion of *GAF1 (YCR016w)* in MCS1 of pETDuet-1	project lab
#728	pETDuet-FLAG-*PRP43*	Amp^R *, FLAG-PRP43* in MCS2 of pETDuet-1	this work
#729	pETDuet-His6-*YCR016w*-FLAG-*PRP43*	Amp^R *, FLAG-PRP43* in MCS2 of pETDuet- His6-*YCR016w*	this work
#812	pETDuet-His6-*PFA1*	Amp^R , His6-tag fusion of *PFA1* in MCS1 of pETDuet-1	this work
#51	pGEX-6P-1	Amp^R, expression vector for *E. coli*, contains the Gst-tag and the PreScission site	GE Healthcare
#826	pGEX-6P-Gst-*TMA23*(FL)	Amp^R, Gst-tag fusion of *E. coli* codon optimized *TMA23*(FL) in pGEX-6P-1, contains PreScission site	this work
#833	pGEX-6P-Gst-*TMA23*(1-61)	Amp^R, Gst-tag fusion of *E. coli* codon optimized *TMA23-Gpatch* in pGEX-6P-1, contains PreScission site	this work
#834	pGEX-6P-Gst-*TMA23*(62-211)	Amp^R, Gst-tag fusion of *E. coli* codon optimized *TMA23ΔGpatch* in pGEX-6P-1, contains PreScission site	this work

Primers used for molecular cloning and sequencing are depicted in table 3. All primers were purchased from Sigma Aldrich. The lyophilized oligonucleotides were solved in *aqua bidest.* Fresenius to a final concentration of 100 pmol/µl.

Table 3: Primers used for molecular cloning and sequencing.

Primer	Sequence (5' →3')	Description
Pfa1_BamH1_Fw	AAAAGGATCCGATGGCAAAAAGGCATAG	forward primer for cloning of *PFA1* into pETDuet-1
Pfa1_Sal1_Rev	AAAAAATCGACTTAACTTTCACTGTGTCTTAAAC	reverse primer for cloning of *PFA1* into pETDuet-1_MCS1
Prp43_Nde1_Flag_Fw	AAAAAACATATGGATTATAAAGATGACGATGACAAAATGGGTTCCAAAAGAAGATTCTCG	includes FLAG-tag, forward primer for cloning of *PRP43* into pETDuet-1_MCS2
Prp43_Xho1_Rev	AAAAAACTCGAGCTATTTCTTGGAGTGCTTACTCTTC	reverse primer for cloning of *PRP43* into pETDuet-1_MCS2 and sequencing
Tma23synth_BamH1_Fw	AAAAAAGGATCCATGGACAGTAAAGA	forward primer for cloning of *E. coli*-codon optimized full length *TMA23* and *E. coli*-codon optimized *TMA23_aa1-61* into pGEX-6P-1
Tma23synth_Rev	AAAAAAGGATCCATGACAAGAAATAGTAG	reverse primer for cloning of *E. coli*-codon optimized full length *TMA23* into pGEX-6P-1
Tma23opt_aa61_Sal1_Rev	TTTTTGTCGACTTAATTCTTGAGGTGTCCGTCGAAC	reverse primer for cloning of *E. coli*-codon optimized *TMA23_aa1-61* into pGEX-6P-1
Tma23opt_aa62_BamH1-Fw	AAAAAGGATCCCTTGACGTGAGCACTGACAGCAATAACGGG	forward primer for cloning of *E. coli*-codon optimized *TMA23_aa62-211* into pGEX-6P-1
Tma23opt_Sal1-Rev	TTTTTGTCGACTTAAATATGTTCTTTACGATC	reverse primer for cloning of *E. coli*-codon optimized *TMA23_aa62-211* into pGEX-6P-1
Prp43_2056Fw	CTGATCCATCCTAGTACGG	forward primer for *PRP43* sequencing
Pfa1_SeqF	CCAGGAAAGATGACTTCTGATG	forward primer for *PFA1* sequencing
Pfa1_seq_F3	GCGAAGCATTATAATATGAAGAG	forward primer for *PFA1* sequencing
Pfa1_269R	CGGCTCTTGGCATCGCGACC	reverse primer for *PFA1* sequencing

2.2 Culture Media

The culture media for *Escherichia coli* as well as for *Saccharomyces cerevisiae* are depicted in table 4. For sterilization all media were autoclaved at 121°C for 20 minutes. Any antibiotic stock solution was added after heat sterilization.

Table 4: Culture media for *Escherichia coli* and *Saccharomyces cerevisiae* used in this study.

***E. coli* culture media**		
2x TY / Agar	16 g/l	tryptone
	10 g/l	yeast extract
	5 g/l	NaCl
	20 g/l	agar-agar
	(100 µg/ml	ampicillin (Roth))
	(40 µg/ml	chloramphenicol)
LB	16 g/l	tryptone
	10 g/l	yeast extract
	10 g/l	NaCl
	(100 µg/ml	ampicillin (Roth))
	(40 µg/ml	chloramphenicol)
***S. cerevisiae* culture media**		
YPD / Agar, pH 5.5	10 g/l	yeast extract
	20 g/l	peptone
	20 g/l	glucose
	20 g/l	agar-agar

2.3 Molecular Cloning

2.3.1 Polymerase Chain Reaction (PCR)

The PCR reaction mix used for cloning is listed in table 5. All primers were ordered from Sigma Aldrich and were diluted to a final concentration of 10 µM. Primer sequences are listed in table 3. As DNA template up to 100 ng plasmid DNA or yeast genomic DNA were used. The PCR conditions are depicted in table 6.

PCR products were analyzed via agarose gel electrophoresis and were purified using the GeneJET Gel Extraction Kit from Thermo Scientific prior to restriction digestion.

Table 5: Composition of the PCR reaction mix.

Component	**Volume [µl]**
Phusion® HF DNA Polymerase (NEB) [2 U/µl]	0.5
5x Phusion® HF Reaction Buffer (NEB)	10
dNTPs [2 mM] (Fermentas)	5
forward primer [10 µM] (Sigma Aldrich)	5
reversed primer [10 µM] (Sigma Aldrich)	5
template DNA	1
aqua bidest. Fresenius	23.5
total	**50**

Table 6: PCR conditions.

Reaction Step	T [°C]	Time	
Initial Denaturation	98	30 sec	
Denaturation	98	10 sec	35 cycles
Annealing	55	30 sec	
Extension	72	60 sec	
Final Extension	72	3.0 min	
Hold	4	∞	

2.3.2 Agarose gel electrophoresis

DNA samples were prepared with DNA Gel Loading Dye (6X) from Thermo Scientific, diluted to a final concentration of 1x. A 1% agarose gel comprising 1 % agarose in 1x TAE buffer and 0.2 µg/ml ethidium bromide was utilized for gel electrophoresis, whereby 0.5x TAE buffer served as running buffer. The composition of 50x TAE buffer is listed in table 7.

Electrophoresis was performed in a Biorad electrophoresis system at a voltage of 80 – 110. As standard marker GeneRuler 1 kb DNA Ladder from Thermo Scientific was used (figure 5). DNA was visualized under UV light using the transilluminator "BIORAD Molecular Imager® Gel Doc™ XR+ with Image Lab Software™".

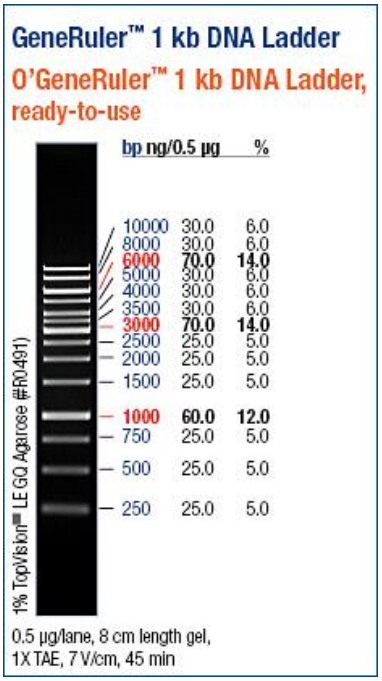

Figure 5: Standard marker GeneRuler 1kb Ladder from Thermo Scientific used for agarose gel electrophoresis.

Table 7: Buffers used for agarose gel electrophoresis.

Buffer	Components	
50x TAE	2 M	Tris/acetate, pH 8.0
	50 mM	EDTA
6x Loading Dye	10 mM	Tris/HCl, pH 7.6
	0.03 %	Xylen Cyalone FF
	0.03 %	Bromphenole blue
	60%	Glycerin
	60 mM	EDTA

2.3.3 Restriction enzyme digestion and ligation

All restriction enzymes (HF) and corresponding buffers used in this study were purchased from NEB and were used according to the recommendations of the company. Digestion was performed at 37°C for one hour. To isolate the desired DNA fragment the total restriction mixture was separated via preparative agarose gel electrophoresis, the corresponding band was cut out using a clean scalpel and DNA was extracted with the GeneJET Gel Extraction Kit from Thermo Scientific. The purification was performed according to the protocol of the company. Digested PCR products were purified via GeneJET Gel Extraction Kit from Thermo Scientific directly after restriction digestion.

Subsequently, ligation was performed using a threefold excess of insert DNA over vector DNA and the T4-DNA-Ligase and corresponding buffer from Thermo Scientific.

The components of the total ligation reaction mix are depicted in table 8. Ligation was carried out for one hour at room temperature or overnight at 16°C. Afterwards the ligation mixture was desalted via drop dialysis for at least 30 minutes prior to electroporation.

Table 8: Composition of the ligation reaction mixture.

Component	Volume [µl]
T4 DNA Ligase [1U/µl] (Thermo Scientific)	0.7
10x T4 DNA Ligase buffer (Thermo Scientific)	1.5
vector DNA	~3 - 10
insert DNA	~3 - 7
aqua bidest. Fresenius	x
total	**15**

2.3.4 Generation of electro-competent *E. coli* XL1 cells

A culture of *Escherichia coli* XL1-blue was inoculated in 500 ml 2x TY and incubated at 37°C and 170 rpm until the culture reached an OD_{600} of 0.5-0.7. The culture was then cooled down on ice for 30 minutes prior to centrifugation at 5000 rpm and 4°C for 7 minutes to harvest the cells. After removing the supernatant by decanting, the cell pellet was resuspended in ice cold sterile 10 % glycerol. Centrifugation at 5000 rpm and 4°C for 7 minutes followed. Cells were washed by repeating the previous step twice. Finally, cells were resuspended in 0.5 to 1 ml ice cold 10 % glycerol and aliquots were rapidly frozen by snap freezing with liquid nitrogen. Electro-competent *E. coli* XL1 were stored at -80°C until use.

2.3.5 Transformation into *E. coli* XL1 via Electroporation

40 µl electro-competent *E. coli* XL1 cell suspension were mixed with 3 µl of the ligation mix or 1 µl of plasmid DNA. The transformation mix was then transferred into UV-sterilized electroporation cuvettes; air bubble formation was avoided. Cuvettes were put into the Multiporator® electroporation system from Eppendorf and electroporation was carried out by applying 2.5 kV pulse for 5 ms. Immediately after the pulse 1 ml of 2x TY media was pipetted into the cuvettes, gently mixed up and down twice and was transferred into a fresh Eppendorf tube. Cells were then regenerated at 37°C at 600 rpm for 30 minutes. Finally, cells were plated on Ampicillin (100 µg/ml) (Roth) containing 2x TY plates and were incubated at 37°C overnight.

2.3.6 Isolation of plasmid DNA from *E. coli* XL1 cells via Mini preparation

2 ml of 2x TY supplemented with 100 µg/ml ampicillin were inoculated with a colony of *E. coli* XL1 transformants and incubated at 37°C and 170 rpm overnight. Cells were harvested by centrifugation at 13000 rpm for 1 minute at room temperature prior to the usage of Thermo Scientific's GeneJET Plasmid Miniprep Kit to isolate plasmid DNA.

To verify the isolated plasmid, restriction analysis was performed. All constructed plasmids were further verified by sequencing (Microsynth).

2.4 Recombinant protein expression in *E. coli* BL21 (DE3) RIL

2.4.1 Generation of $CaCl_2$ competent *E. coli* BL21 (DE3) RIL cells

50 ml 2x TY with Chloramphenicol (40 µg/ml) were inoculated with *E. coli* BL21 (DE3) RIL to an OD_{600} of 0.05 and were incubated at 37°C and 170 rpm until the culture reached an OD_{600} of 0.3 - 0.4. The cell culture was then cooled down on ice for 30 minutes prior to the cell harvest by centrifugation at 4000 rpm for 8 minutes at 4°C. After removing the supernatant by decanting, the cell pellet was resuspended in 10 ml of ice cold 100 mM $CaCl_2$. Centrifugation at 3500 rpm for 5 minutes at 4°C followed. To wash the cells the previous step was repeated. After removing the supernatant, cells were resuspended in 0.5 to 1 ml ice cold 100 mM $CaCl_2$ with 15 % Glycerol. Aliquots of the cell suspension were rapidly frozen by snap freezing with liquid nitrogen. $CaCl_2$ competent *E. coli* BL21 (DE3) RIL were stored at -80°C until use.

2.4.2 Transformation into $CaCl_2$ competent *E. coli* BL21 (DE3) RIL cells

40 µl of $CaCl_2$ competent *E. coli* BL21 (DE3) RIL cell suspension were mixed gently with 10-100 ng plasmid DNA. The transformation mixture was incubated on ice for 30 minutes prior to heat shock at 42°C in the water bath for 2 minutes. For regeneration 900 µl of 2x TY media were added and incubation at 37°C in the water bath for 45 minutes followed. Afterwards cells were plated on Ampicillin (100 µg/ml) and Chloramphenicol (40 µg/ml) containing 2x TY plates and were incubated at 37°C overnight.

2.4.3 Cell culturing and harvesting for recombinant protein expression

E. coli BL21 (DE3) RIL containing the corresponding expression plasmid were grown overnight in LB media supplemented with 100 µg/ml Ampicillin and 40 µg/ml Chloramphenicol. This preculture was then diluted 1:200 in fresh LB media with Ampicillin (50 µg/ml) and was inoculated at 37°C and 170 rpm. When the culture reached an OD_{600} of 0.3 - 0.4 it was shifted to 16°C in a shaking water bath. After 30 minutes protein expression was induced by adding 0.3 mM IPTG for 20 hours.

Cells were harvested by centrifugation at 5000 rpm and 4°C for 10 min using BECKMAN COULTER Avanti® Centrifuge J-26 XP. The supernatant was removed by decanting and cell pellets were resuspended with ice cold ddH_2O. Centrifugation at 4000 rpm and 4°C for 15

minutes followed using Eppendorf Centrifuge 5810R. The supernatant was decanted and the cell pellets were stored at -20°C until use.

2.5 Purification of recombinant proteins expressed in *E. coli* BL21 (DE3) RIL

After harvesting the cells, cell pellets were resuspended in 1.5x volume of lysis buffer and incubated for 40 minutes on ice. Cells were lysed by sonication (three times for 13 milliseconds with an amplitude of 35 %) using BRANSON Digital Sonifier. To remove cell debris and insoluble proteins centrifugation at 19000 rpm and 4°C for 30 minutes was performed.

For FLAG-Prp43 purification the supernatant was incubated with equilibrated ANTI-FLAG® M2 affinity Gel from Sigma Aldrich (0.6 ml/L cell culture) for 1 hour on a turning wheel at 4°C to allow protein binding. Four washing steps with buffer containing 50 mM Tris/HCl pH 7.5, 500 mM NaCl, 1 mM DTT and 0.05% Nonidet P40 Substitute and centrifugation at 4000 rpm and 4°C for 2 minutes followed. The fifth washing step was carried out with 150 mM instead of 500 mM NaCl to reduce the salt concentration for further experiments. FLAG-Prp43 was then eluted with FLAG peptide from Sigma Aldrich according to the company's instructions. If further purification via Size Exclusion Chromatography (SEC) followed, elution was performed overnight on a turning wheel at 4°C.

For His6-Pfa1 purification the supernatant was incubated with equilibrated Ni-NTA agarose beads from Qiagen (0.3 ml/L cell culture) for 1 hour at 4°C on a turning wheel to allow protein binding. After washing (same washing steps as for FLAG-purification) with buffer supplemented with Imidazole, beads were incubated with buffer containing 300 mM Imidazole for 20 minutes at 4°C on a turning wheel to elute His-Pfa1.

For GST-purification the supernatant was incubated with Glutathione Agarose from Sigma Aldrich (10 mg/L cell culture) for 1 hour on a turning wheel at 4°C to allow protein binding. After washing (same washing steps as for FLAG-purification) beads were incubated with buffer containing 10 mM glutathione on a turning wheel at 4°C for 20 minutes. If further purification via SEC followed, elution was performed overnight on a turning wheel at 4°C.

If needed, eluates were concentrated using Amicon® Ultra-4 Centrifugal Filter Units from Millipore according to the company's instruction manual.

For storage at -80°C glycerol was added to the eluates to a final concentration of 7%.

Table 9: Buffers used for purification of recombinant proteins.

Buffer	Component
Lysis Buffer	50 mM Tris/HCl, pH 7.5 500 mM NaCl 1 mM DTT 0.5 mM PMSF (phenyl-methyl-sulfonyl-fluorid) 1x Protease-Inhibitor Mix HP (SERVA) 1 mg/ml Lysozyme (ROTH) 0.05 % Nonidet P40 Substitute (USB Corporation) 40 mM Imidazole (just for His6-Pfa1 purification)
Equilibration Buffer	50 mM Tris/HCl, pH 7.5 500 mM NaCl
Wash Buffer 1	50 mM Tris **500 mM NaCl** 1 mM DTT 40 mM Imidazole (just for His-purification)
Wash Buffer 2	50 mM Tris **150 mM NaCl** 1 mM DTT 40 mM Imidazole (just for His-purification)
FLAG-tag Elution Buffer	50 mM Tris/HCl, pH 7.5 150 mM NaCl 1 mM DTT 100 µg/ml FLAG peptide
His6-tag Elution Buffer	50 mM Tris/HCl, pH 7.5 150 mM NaCl 300 mM Imidazole 1 mM DTT
GST-tag Elution Buffer	50 mM Tris/HCl, pH 7.5 500 mM NaCl 10 mM Glutathione 1 mM DTT

When GST-tagged proteins were further purified with SEC, RNase A (1:1000 the volume of the supernatant) from Thermo Scientific's GeneJET Plasmid Miniprep Kit was added to the supernatant and was incubated for 10 minutes at 4°C under rotation prior to the incubation with the glutathione agarose beads.

2.5.1 Size Exclusion Chromatography (SEC)

SEC was carried out using the Superdex 200 Increase 10/300 GL column from GE Healthcare Life Sciences. The compositions of the buffers used for SEC are depicted in table 10.

Table 10: Composition of SEC running buffers.

Component	Concentration
SEC of FLAG-Prp43	
Tris/HCl pH 7.5	25 mM
NaCl	150 mM
$MgCl_2$	10 mM
DTT	0.2 mM
SEC of Gst-Tma23(FL)(1-61)(62-211), Gst	
Tris/HCl pH 7.5	50 mM
NaCl	500 mM

Pooled fractions were concentrated using Amicon® Ultra-4 Centrifugal Filter Units from Millipore according to the company's instruction manual.

2.5.2 Determination of protein concentration via Bradford Assay

To determine the protein concentration in the eluates the Bradford Protein Assay from BIORAD was used. The Bradford Reagent was brought to room temperature before use. To prepare the reagent one part of the reagent concentrate was diluted with four parts of *aqua bidest.* (Fresenius). For one reaction 3 ml of the diluted reagent was mixed with 100 µl of the protein sample, comprising 5 µl of the eluate and 95 µl *aqua bidest.* (Fresenius), in a cuvette and incubation at room temperature for 5 minutes followed. The absorbance at 595 nm was measured using the Beckman DU® 640 spectrophotometer. A bovine serum albumin standard curve ($y = 0.0168x - 0.0008$), which was measured with the same spectrophotometer, was used for the calibration of the protein concentration.

2.5.3 Buffer exchange

To remove any interfering compounds like Imidazole and to reduce the salt concentration for the ATPase assays a buffer exchange was performed. Therefore Zeba™ Spin Desalting Columns from Thermo Scientific were used and the procedure was performed according to the company's instruction manual.

2.6 SDS-polyacrylamide gel electrophoresis (SDS-PAGE)

For SDS-PAGE NuPAGE® Novex® 4-12% Bis-Tris Gels (Thermo Scientific) with NuPAGE® MOPS Running Buffer were used.

All samples were denatured by adding final sample buffer (FSB) to a final concentration of 2.5x prior to incubation at 95°C for 10 minutes followed by centrifugation at 13000 rpm and room temperature for 1 minute. The composition of 5x FSB is depicted in table 11.

Table 11: Composition of FSB (final sample buffer) used for SDS-PAGE.

Buffer	Component
5x FSB (final sample buffer)	0.3 M Tris/HCl, pH 6.6
	0.5 M DTT
	50 % glycerol
	10 % SDS
	0.02 % bromphenol blue
Fixing solution	50 % methanol
	10 % acetic acid

To determine the molecular weight of the proteins PageRuler™ Prestained Protein Ladder (10 to 170 kDa) from Thermo Scientific was applied as standard marker (figure 6).

Electrophoresis was performed with a voltage of 100-160 in the XCell SureLock™ Mini-Cell Electrophoresis System from Thermo Scientific.

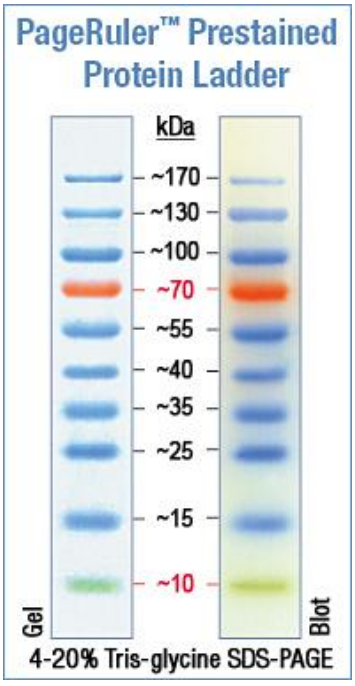

Figure 6: Standard marker PageRuler Prestained™ Protein Ladder, 10 to 170 kDa from Thermo Sientific used for SDS-PAGE.

For protein staining the Colloidal Blue Staining Kit from Thermo Scientific was used. The polyacrylamide gel was incubated in fixing solution (table 11) for 10 minutes on a shaker prior to incubation with stainer solution A (4 ml Stainer A, 4 ml methanol and 12 ml deionized water) for 10 minutes before 1 ml of Stainer B was added. The gel was incubated with staining solution overnight. Incubation with deionized water for at least 7 hours followed to clear the background.

2.7 Western blotting

After separating the proteins using SDS-PAGE, proteins were transferred to a PVDF membrane (Millipore) via electro transfer at 220 mA for two hours using the Trans-BlotTMCell system from Biorad. The composition of the utilized transfer buffer is depicted in table 13. The membrane was blocked overnight in 1x TST-buffer with 0.5 % milk powder or for 30 minutes in 1x TST-buffer with 2 % milk powder on a shaking plate at 4°C. For detection of GST-tagged proteins the membrane was incubated with the α-Gst antibody for one hour, thereafter was washed three times with 1x TST for 5 minutes before the incubation with the secondary antibody (goat-α-rabbit, HRP) followed. For the detection of FLAG-Prp43 and His6-Pfa1 the membrane was incubated with conjugated antibodies (α-FLAG and α-His6 with horseradish peroxidase) for 1 hour. All antibodies were diluted in 1x TST buffer. The dilution and the origin of the used antibodies are listed in table 12.

Table 12: Antibodies used in this study.

Antibody	Dilution	Origin
α-FLAG (conjugated)	1:15000	Sigma Aldrich
α-His6 (conjugated)	1:10000	Sigma Aldrich
α-Gst	1:5000	Sigma Aldrich
goat-α-rabbit, HRP	1:15000	Sigma Aldrich

To remove unbound antibody the membrane was washed three times with 1x TST prior to detection via chemiluminescence using the ECL-chemiluminescence kit from Biorad. The membrane was incubated in a 1:1 mixture of ECL solution 1 and 2 for 2 minutes. The membrane was imaged by using ChemiDoc^{TM} Touch Imaging System from Biorad.

To remove the antibody the membrane was incubated in stripping buffer at 55°C for 20 minutes. Afterwards the membrane was rinsed with ddH_2O two times followed by three washing steps with 1x TST for 5 minutes. The components of the buffers used for western blotting are listened in table 13.

Table 13: Buffers used for western blotting.

Buffer	Component	
Transfer buffer	48 mM	Tris pH 8.3
	390 mM	Glycine
	20%	methanol
	0,1 %	SDS
1x TST buffer	50 mM	Tris/HCl, pH 7.4
	0.1 %	Tween20
	0.15 %	NaCl
Stripping buffer	60 mM	Tris/HCl, pH 6.8
	2 %	SDS
	100 mM	β-mercaptoethanol

2.8 *In vitro* interaction assay between GST-Tma23 and FLAG-Prp43

Recombinant proteins from 500 ml *E. coli* BL21 culture were purified according to the protocol outlined in section 2.5. Prey proteins were added to the bait protein immobilized on beads. Incubation for 1 hour at 4 °C on a turning wheel followed. Subsequently, unbound proteins were removed by 5 washing steps using 500 µl buffer containing 50 mM Tris/HCl pH 7.5, 150 mM NaCl and 1 mM DTT. Proteins were eluted using FLAG-peptide or glutathione buffer (table 9). SDS-PAGE and Coomassie blue staining as well as western blotting was performed to analyze the eluates.

2.9 *In vitro* interaction assay between His6-Gaf1 and FLAG-Prp43

His-Gaf1 and FLAG-Prp43 were co-expressed from the pETDuet-1 vector (500 ml culture) and cells were harvested according to the protocol outlined in section 2.4.3. Subsequently, proteins were purified via two-step purification following the FLAG- and His- purification protocol described in section 2.5, using lysis and washing buffer that contained 150 mM NaCl. When FLAG-purification was performed first, the FLAG-eluate was subjected to the His-purification protocol. For the inverse experiment, His-purification was carried out prior to FLAG-purification. SDS-PAGE and Coomassie blue staining as well as western blotting was carried out to analyze the eluates.

2.10 ATPase Assay (Malachite green phosphate assay)

FLAG-Prp43 and the G-patch proteins were purified according to the protocol outlined in section 2.5.

The protein concentrations of the protein solutions used for the ATPase assay were determined using the Bradford Assay (section 2.5.2.). The ATPase activity of FLAG-Prp43 was determined in a reaction volume of 100 µl. The applied amounts of FLAG-Prp43, G-patch proteins, ATP and total yeast RNA (for RNA isolation see section) for one reaction are depicted in table 14.

Table 14: Concentration of applied proteins, ATP and total yeast RNA for one reaction of the ATPase assay with a total volume of 100 µl.

Component	Concentration
RNA helicase	100 nM
G-patch protein	500 nM
RNA	150 µM
ATP	1 mM

A phosphate standard curve was generated according to the company's instruction manual.

The reaction mixtures were prepared on ice and mixed by vortexing, before they were incubated at 37°C for 30 minutes in a water bath for ATP hydrolysis. Prior to the assay, the reaction mixtures were diluted and 20 µl of the working reagent were transferred to separate wells of a 96 well microtiter plate. To perform the assay 80 µl of each dilution were added to the working reagent – which had been prepared according to the company's instruction manual – mixed and incubated for 30 minutes at room temperature for color development. Subsequently, the absorbance at an OD of 600 nm was measured in the TECAN GENiosPro reader using the XFluor4GeniosPro software. The composition of the buffer used for the ATPase assay is depicted in table 15.

Table 15: Buffer used for the ATPase assay.

Component	Concentration
Tris/HCl pH 7.5	25 mM
NaCl	150 mM
$MgCl_2$	10 mM
DTT	0.2 mM

2.10.1 Isolation of total yeast RNA using RNeasy Mini Kit from Qiagen

100 ml of YPD media were inoculated with a colony of *S. cerevisiae* W303 strain and were grown to an OD_{600} of 0.5 - 0.8 at 30°C and 170 rpm. Subsequently, cells were harvested by centrifugation at 1000 g 5 minutes and 4°C. The supernatant was removed by decanting, cell pellets were put on ice and were resuspended with ice cold ddH_2O. A further centrifugation step followed, the supernatant was removed completely and cell pellets were stored at -20°C until use.

For mechanical disruption cells were resuspended in 1.2 ml of RLT buffer containing 12 µl of β-mercaptoethanol. 600 µl of acid-washed glass beads were transferred into 2 ml screw cap vial. Afterwards, the cell suspension was split and each half was added to the glass beads. Cells were disrupted by agitating for 3 minutes using Biospec Products Mini-Beadbeater™. After cell disruption beads were pelleted by centrifugation at 13000 rpm for 1 minute at 4°C. Subsequently, 100 % ethanol was added to the homogenized lysate to a final concentration of 35 %.

The RNA isolation from the lysate was then performed according to the RNeasy Mini Handbook 06/2012, pages 48 - 49. After elution the RNA concentration was determined using NanoDrop from Thermo Scientific and finally, RNA was stored at -20 °C until use.

2.11 Dot spot assay

Strains were grown on YPD plates for one day, strains containing a *PXR1* deletion for two days at 30°C. Cells were resuspended in YPD media and diluted to an OD_{600} of 0.5. 250 µl of the suspensions were pipetted into a 96 well microtiter plate and diluted in 1:10 steps to a dilution of 10^{-4}. Finally, cell suspensions were spotted on three YPD plates and incubated at 25°C, 30°C and 37°C.

3 Results

3.1 Tma23 binds directly to the RNA helicase Prp43

G-patch proteins were shown to directly interact with their helicase partners. Yeast-two-hybrid experiments performed by Dieter Kressler revealed that Tma23 interacts with the RNA helicase Prp43 (Kressler D., unpublished). Furthermore a fragment between amino acid 71 and 110 was identified as minimal interaction surface and was shown to contain a motif conserved to the previously identified Prp43 interaction surface of Pxr1 (Banerjee et al., 2015) (figure 7). Thus, this motif was termed *Prp43 interaction motif*, PIM (Kressler D., unpublished).

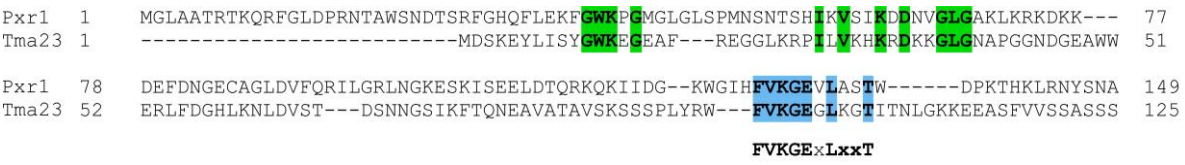

Figure 7: Sequence alignment of Pxr1 and Tma23. Conserved residues within the G-patch are shaded in green, Conserved residues within the PIM (Prp43 interaction motif) (Dieter Kressler, unpublished) are shaded in blue. The consensus of the PIM is indicated. The PIM is located within the minimal Prp43 interaction surface of both Pxr1 and Tma23. (Aligned with Cobalt, NCBI)

To confirm these results, we performed an *in vitro* interaction assay using recombinant proteins expressed in *E. coli* BL21 and tested the full-length Tma23 and two truncated versions for their Prp43 binding ability. Since full-length His-tagged Tma23 could not be expressed in *E. coli* a codon-optimized Tma23 sequence was used for recombinant protein expression. GST- instead of His-tagging helped to obtain sufficiently soluble protein (full-length as well as truncated versions) for protein purification using glutathione agarose. FLAG-tagged Prp43 was purified with agarose beads coated with monoclonal anti-FLAG antibodies. For the *in vitro* interaction assay purified full-length GST-Tma23(FL) or the truncated versions GST-Tma23(1-61) and GST-Tma23(62-211) were incubated with FLAG-Prp43 bound to the anti-FLAG agarose beads. After stringent washing and elution FLAG-eluates were analyzed by SDS-PAGE followed by Coomassie blue staining and western blotting using anti-FLAG and anti-GST antibodies. If the proteins are directly interacting one would expect that the full-length GST-Tma23 occurs in the FLAG-eluate. Since the yeast-two-hybrid test showed that the minimal interaction fragment is located between amino acids 71 and 110, also GST-Tma23(62-211) should bind to FLAG-Prp43 *in vitro* and should be obtained in the FLAG-eluate, while GST-Tma23(1-61) should not (figure 8a).

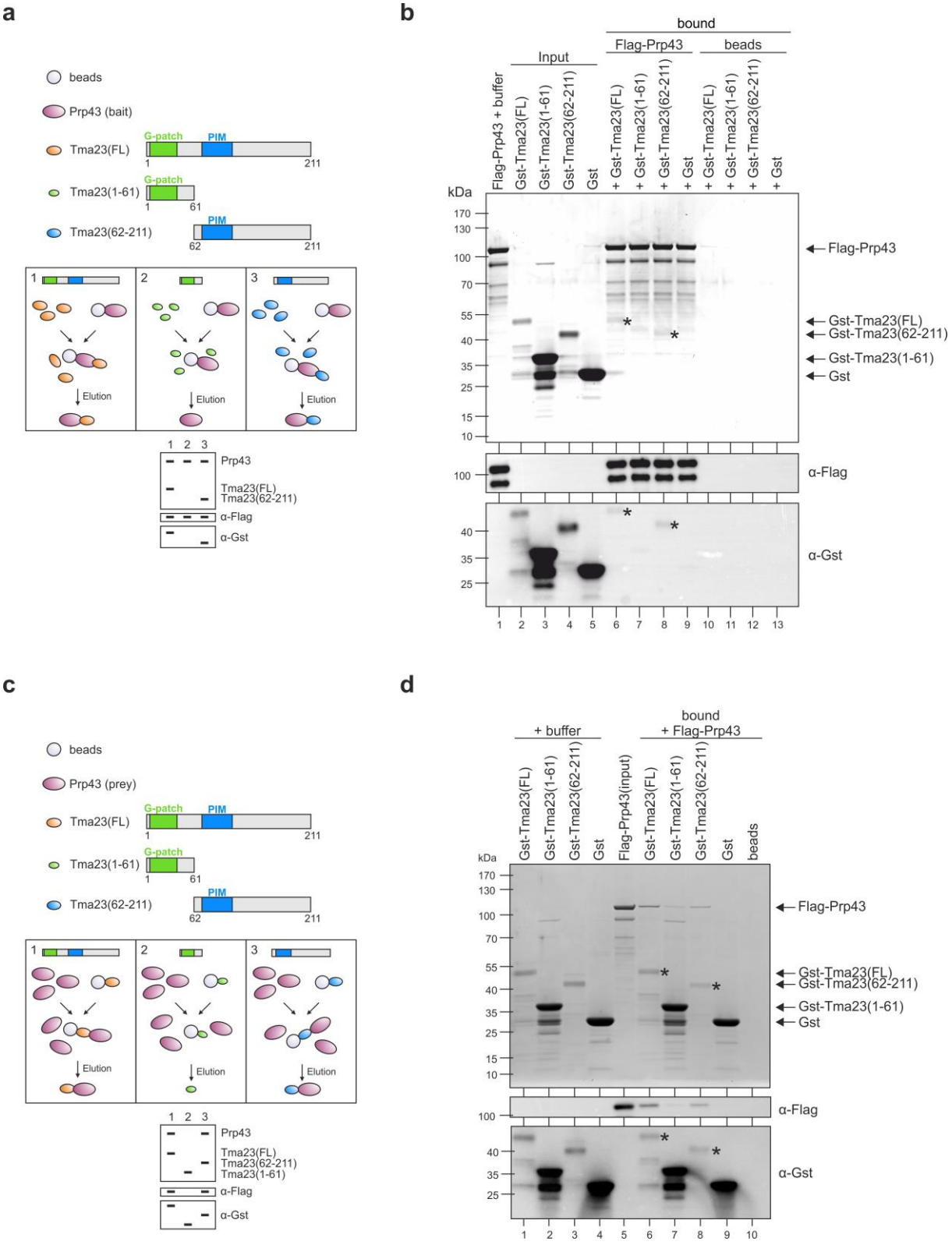

Figure 8: Direct interaction of Tma23 and Prp43 *in vitro*. (a) Experimental scheme of the *in vitro* interaction assay using FLAG-Prp43 as bait (bound) and GST-Tma23 variants as prey proteins. FLAG-Prp43 was immobilized on anti-FLAG beads and was incubated with purified GST-Tma23(FL), GST-Tma23 truncations or buffer. After stringent washing and elution, eluates were analyzed with SDS-PAGE and Coomassie staining as well as western blotting using the indicated antibodies. If the PIM of Tma23 indeed provides the main Prp43 interaction surface, GST-Tma23(FL) and GST-Tma23(62-211) should be recovered in the FLAG-eluate, while

Tma23(1-61) should not. **(b)** Only GST-Tma23 variants containing the PIM directly interact with FLAG-Prp43. The direct interaction between FLAG-Prp43 and GST-Tma23 variants was investigated using the protocol outlined in (a) Bound proteins are indicated by asterisks. **(c)** Experimental scheme of the inverse experiment to (a) using GST-Tma23 variants as bait and FLAG-Prp43 as prey protein. GST-Tma23 variants were immobilized on glutathione agarose beads and each was incubated with purified FLAG-Prp43 or buffer. Again, only GST-Tma23 variants that contain the PIM should bind FLAG-Prp43. **(d)** GST-Tma23(FL) and GST-Tma23(62-211) co-precipitate FLAG-Prp43, while GST-Tma23(1-61) that lacks the PIM does not. The experimental procedure is depicted in (c). Bound proteins are indicated by asterisks.

GST-Tma23(FL) directly binds to FLAG-Prp43 (figure 8b, lane 6) and the interaction is specific, since no GST-Tma23(FL) is obtained when mixed with empty anti-FLAG beads (figure 8b, lane 10). In contrast, GST-Tma23(1-61), which contains the G-patch but lacks the PIM, shows no *in vitro* interaction with the helicase (figure 8b, lane 7). However, GST-Tma23(62-211) containing the PIM binds specifically to FLAG-Prp43, since GST-Tma23(62-211) only appears in the FLAG-eluate when added to FLAG-Prp43 coated beads (figure 8b, lane 8), but not when added to the empty ones (figure 8b, lane 12).

To further confirm these observations, we performed the inverse experiment using GST-Tma23(FL) or the truncated versions as bait protein bound to glutathione agarose beads, while purified FLAG-Prp43 was added as prey protein. Again, only in case of a direct interaction between the two tested proteins both appear in the eluate (figure 8c). As expected, FLAG-Prp43 directly interacted with GST-Tma23(FL) (figure 8d, lane 6) and GST-Tma23(62-211) (figure 8b, lane 8). In this assay also GST-Tma23(1-61) lacking the PIM bound low amounts of FLAG-Prp43 (figure 8d, lane7). However, this results from the unequal amount of bait protein that was loaded onto the gel. If one would load as much bait protein as in the lanes 6 or 8, where the amount of the bait protein is much lower, the band of FLAG-Prp43 would not be visible anymore. This suggests a transient interaction between FLAG-Prp43 and the G-patch domain of Tma23, which is not surprising, since the G-patch is known to transiently interact in course of stimulation of the helicase.

These findings confirmed the results from the yeast-two-hybrid test and we can conclude that Tma23 directly binds to Prp43. Furthermore, we showed that the G-patch domain of Tma23 is not sufficient for the stable interaction with Prp43 like it is known for other G-patch proteins (Chen et al., 2014; Heininger et al., 2016; Lebaron et al., 2009; Silverman et al., 2004; Tanaka et al., 2007; Tsai et al., 2005). We conclude that Tma23 contains a domain distinct from the G-patch that harbors the ability to interact with Prp43 and contains the PIM.

3.2 Does GST-Tma23 stimulate the ATPase activity of FLAG-Prp43?

It was previously shown that the G-patch proteins Ntr1, Pfa1, Pxr1 and Cmg1 stimulate the otherwise weak ATPase activity of Prp43 (Chen et al., 2014; Christian et al., 2014; Heininger

et al., 2016; Lebaron et al., 2009). To investigate whether Tma23 is also able to stimulate the ATPase activity of Prp43 we aimed to perform an ATPase assay. For this purpose we purified recombinant GST-Tma23 and FLAG-Prp43 and used the Malachite Green Phosphate Assay to determine the ATPase activity of Prp43 in presence and absence of GST-Tma23. This assay is based on the color complex formation between Malachite Green, molybdate and free phosphate that can be quantified by measuring the absorbance at 600 nm.

3.2.1 Pretesting of buffer conditions and protein concentrations for the ATPase assay

We performed a pretest to estimate suitable protein and RNA concentration as well as buffer conditions. Therefore, we purified recombinant FLAG-Prp43 and GST-Tma23 expressed in *E. coli* BL21 using FLAG- and GST-purification. SDS-PAGE followed by Coomassie staining was performed to check the purity of the protein preparations. Subsequently, the ATPase activity of Prp43 in dependency of Tma23 was determined using the Malachite Green Phosphate Assay. To test whether FLAG-Prp43 from our preparation can be stimulated we also determined the ATPase activity in presence of RNA as a positive control, because it is known that RNA causes the stimulation of the ATPase activity of Prp43 (Chen et al., 2014; Lebaron et al., 2009; Martin et al., 2002; Walbott et al., 2010). After incubation two different dilutions (1:2 and 1:10) were measured.

The pretest showed ATPase activity of FLAG-Prp43 with the given conditions and the increased amounts of FLAG-Prp43 showed increased activity (figure 9). Furthermore, the addition of total yeast RNA increased the ATPase activity, which suggests successful stimulation of FLAG-Prp43. The addition of GST-Tma23 also led to a stimulation of the ATPase activity of FLAG-Prp43, whereby GST-Tma23 did not hydrolyze ATP on its own (data not shown). When higher concentrations of GST-Tma23 were added the activity was further increased. The highest stimulation occurred when GST-Tma23 was added in addition to RNA. This indicates that both GST-Tma23 and RNA can synergistically stimulate the ATPase activity of Prp43.

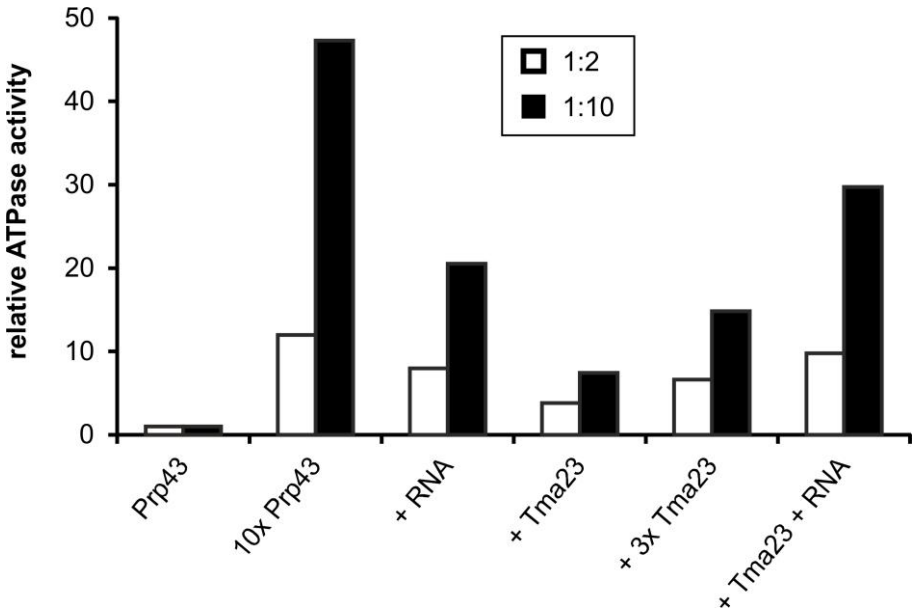

Figure 9: Pretest to measure the ATPase activity of Prp43 stimulated by Tma23 using the Malachite Green Phosphate Assay. The relative ATPase activity of FLAG-Prp43 [100 nM] in presence or absence of total yeast RNA [150 µM] and/or GST-Tma23 [~ 250 nM] is indicated (protein and RNA concentration as in (Walbott et al., 2010)). The ATPase assay was performed in a buffer containing 25 mM Tris/HCl pH 7.5, 10 mM $MgCl_2$ and 0.2 mM DTT (adapted from (Chen et al., 2014)). After incubation for 30 minutes at 37°C for ATP hydrolysis the mixtures were diluted (1:2 and 1:10). Dilutions were mixed with the working reagent and incubation for 30 minutes followed. Subsequently, the absorbance at an OD of 600 nm was measured in duplicates.

However, the assay revealed an unexpected result. Since the relative and not the absolute ATPase activities are depicted in figure 9 one would expect the same value for both dilutions per sample. However, the 1:10 dilution showed much higher values than the 1:2 dilution. We suspected that the absorbance of the 1:10 dilutions had been too low for an accurate measurement, because the OD_{600} values ranged between 0.07 and 0.3. Moreover, the 1:2 dilution showed a tenfold increase of the activity of FLAG-Prp43 when applying ten times the amount of the helicase in contrast to the 1:10 dilution that revealed a fiftyfold increase. That indicated that the values from the 1:2 dilution were more reliable.

All in all one can observe the tendency that addition of GST-Tma23 indeed stimulated the ATPase activity of FLAG-Prp43. To exclude that the observed stimulation comes from the GST tag and not from Tma23 we included recombinant GST expressed in *E. coli* BL21 as negative control. Although we again observed a stimulation of the ATPase activity when GST-Tma23 was added, also GST alone stimulated the activity of FLAG-Prp43, but did not hydrolyze ATP alone (data not shown). For this reason we supposed that an *E. coli* protein contamination stimulated the ATPase activity of FLAG-Prp43. Hence, we decided to perform size exclusion chromatography to further increase the purity of the preparations after FLAG- or GST-purification.

3.2.2 Optimization of the GST-Tma23 purification

To remove any *E. coli* protein contaminations that might remain after GST- or FLAG-purification we performed size exclusion chromatography (SEC). However, GST and GST-Tma23 eluted in the size range of aggregates, requiring further optimization of the whole purification process. Increasing the NaCl concentration in the buffer from 150 to 500 mM did not prevent aggregate formation.

Then we reflected on the biochemistry of the protein and its unusually high content of lysines (23.7 %!) that results in a very high isoelectric point (IEP = 11). We suspected that Tma23 very likely binds to negatively charged components i.e. to nucleic acids which might be the cause for aggregation. Hence, we used RNase A for RNA degradation and subsequently purified GST-Tma23 as well as GST using glutathione agarose beads followed by SEC. Indeed, RNase A treatment helped to solubilize the protein, which was why the GST-Tma23 now eluted later, with about 13 ml corresponding to the size of approximately 50 kDa (figure 10).

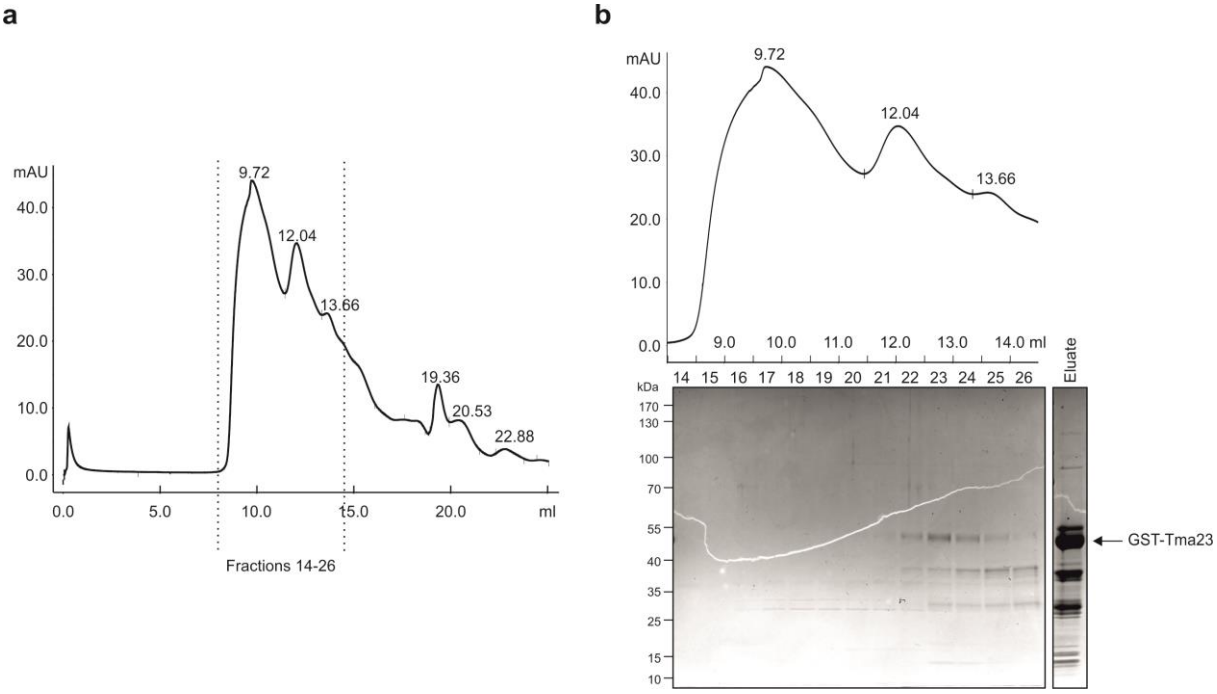

Figure 10: The optimized GST-purification protocol with RNase A treatment provides soluble GST-Tma23 after Size Exclusion Chromatography (SEC). (a) SE-Chromatogram of GST-Tma23 purified via optimized GST-purification with RNase A treatment. The SEC was performed in 50 mM Tris/HCl pH 7.5, 500 mM NaCl using the Superdex 200 Increase 10/300 GL column. The fractions 14-26 were analyzed using SDS-PACE followed by Coomassie blue staining. **(b)** Analysis of the fractions 14-26 of the SEC depicted in (a) using SDS-PAGE followed by Coomassie blue staining. A sample of the GST-eluate from the optimized GST-purification served as reference. As expected according to its molecular weight, GST-Tma23(FL) elutes with approximately 13 ml.

In summary, we were able to optimize the GST-Tma23 purification, using RNase A treatment during GST-purification to avoid protein aggregation, and obtain pure and soluble protein.

3.2.3 GST-fusions of Tma23 truncations showed no significant difference in the stimulation of the ATPase activity of Prp43 in contrast to the full-length protein

With the optimized protein purification protocol in our hands we also decided to purify the truncated versions of Tma23 used for the *in vitro* interaction studies for the ATPase assay. Thereby, both truncations should serve as negative controls. Tma23(1-61) containing the G-patch - the stimulating domain - lacks the interaction surface that harbors the PIM and does not bind to Prp43 efficiently. In contrast, as our interaction studies revealed, Tma23(62-211) containing the interaction surface forms a stable complex with Prp43, but should not be able to stimulate Prp43, because it harbors no activating G-patch domain.

We purified recombinant GST-Tma23(FL) and the two truncations GST-Tma23(1-61) and GST-Tma23(62-211) using the optimized GST-purification protocol followed by SEC. However, the protein yield was far too low for the ATPase assay with the exception of the GST-Tma23(1-61) purification, which provided enough protein.

To test whether there is a benefit using SEC at all, we compared the ATPase stimulation by GST-Tma23(1-61) that was further purified with SEC (“GST-Tma23(1-61)-SEC”) and GST-Tma23(1-61) without further purification (“GST-Tma23(1-61)-w/o”). We supposed that a higher concentration of GST-Tma23(1-61) should lead to a stimulation of Prp43, because the protein transiently binds Prp43. This is also indicated by the *in vitro* interaction study that showed that a higher concentration of Tma23(1-61) led to a weak interaction with FLAG-Prp43, while lower amounts of the co-factor don’t bind to the helicase efficiently (figure 8). Therefore, we also wanted to test the stimulation by increased amounts of GST-Tma23(1-61). Additionally, we also used GST as a negative control. GST and GST-Tma23(1-61) were purified using the optimized protein purification protocol, whereby 100 µl of the GST-Tma23(1-61) eluate were not further purified with SEC. Recombinant His-Pfa1 served as positive control. The mixtures were again diluted before they were subjected to the assay, but this time the mixtures were diluted 1:2 and 1:5 to avoid too low OD_{600} values. Note that we added 150 mM NaCl to the ATPase buffer in contrast to the assay above, because we speculated that higher salt concentration would lead to a better solubility of the proteins.

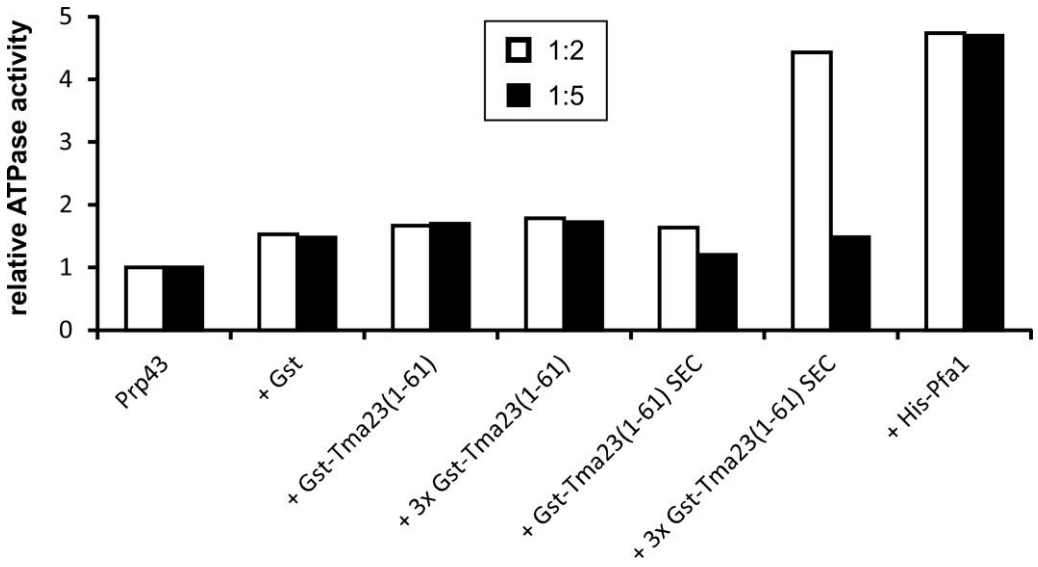

Figure 11: Comparison of GST-Tma23(1-61) purifications with and without following size exclusion chromatography (SEC). The relative ATPase activity of FLAG-Prp43 [100 nM] in presence or absence of GST-Tma23(1-61) [~ 500 nM], GST [~ 500 nM] or His-Pfa1 [~500 nM] is indicated. The ATPase assay was performed in a buffer containing 25 mM Tris/HCl pH 7.5, 150 mM NaCl, 10 mM $MgCl_2$ and 0.2 mM DTT. Gst was purified using glutathione agarose beads and followed by SEC. GST-Tma23(1-61) was also purified with glutathione agarose beads, whereby 100 µl of the eluate were not subjected to the SEC to compare the two preparations in the ATPase assay. His-Pfa1 was purified via His-purification and no buffer exchange was performed. After incubation for 30 minutes at 37°C for ATP hydrolysis the mixtures were diluted (1:2 and 1:5). Dilutions were mixed with the working reagent and incubation for 30 minutes followed. Subsequently, the absorbance at an OD of 600 nm was measured in duplicates.

His-Pfa1 caused a fivefold increase of ATP hydrolysis. His-Pfa1 alone displayed no ATPase activity (data not shown). Addition of GST slightly increased the activity of FLAG-Prp43. The same stimulation was observed after addition of GST-Tma23(1-61)-w/o, while the protein alone did not hydrolyze ATP (data not shown). Addition of a threefold higher concentration of GST-Tma23(1-61) preparation led only to a minor increase of the ATPase activity. The GST-Tma23(1-61) truncation that was further purified with SEC also slightly stimulated FLAG-Prp43, while it showed no ATPase activity on its own (data not shown). In contrast to the ATPase assay above, in this case the dilutions showed the same relative ATPase activities per sample, which is a hint that the values were reliable. However, the relative ATPase activities, when adding a threefold higher concentration of GST-Tma23(1-61) purified with SEC, displayed very different values for the two dilutions. While the 1:2 dilution showed a great stimulation of the ATPase activity, the 1:5 dilution revealed stimulation in the range of the other samples. This difference can only be explained by pipetting errors. However, this result makes it impossible to interpret whether GST-Tma23(1-61) indeed stimulates the ATPase activity of FLAG-Prp43 when using higher concentrations of the G-patch domain and whether this stimulation is Tma23 specific.

To conclude, GST as well as GST-Tma23(1-61), both further purified with SEC did not stimulate the ATPase activity of FLAG-Prp43 significantly, while His-Pfa1 fivefold increased

the ATP hydrolysis of the helicase. Furthermore, there was no significant difference between the two protein preparations of GST-Tma23(1-61). However, the fact, that the 1:2 dilution of the 3x GST-Tma23(1-61)-SEC sample showed an intense stimulation of the ATPase activity, might be an indication that the G-patch domain of Tma23 indeed stimulates the helicase when high amounts of the G-patch are present, even despite the lack of the main Prp43 interaction surface. However, to prove this speculation one has to repeat the experiment using a titration series with different concentrations of the co-factor.

Since aggregation of GST-Tma23 was prevented by RNase treatment, but the amounts of GST-Tma23(FL) and GST-Tma23(62-211) recovered after SEC were not sufficient to perform ATPase assays, we performed another assay with the affinity purified proteins without further purification via SEC, using the GST-fusions of the Tma23 truncations as negative controls. To compare the amounts of protein that were used for the assay, we performed a SDS-PAGE and loaded the same volumes of the protein eluates that were used for an ATPase reaction with a volume of 100 µl.

Note that again the distinct dilutions showed different relative ATPase activities (figure 11). Hence, one has to be particularly careful with the interpretation of these results. Only the reaction with five times the amount of FLAG-Prp43 showed the same relative ATPase activity for both dilutions. However, addition of His-Prp43 stimulated the ATPase activity, while the G-patch protein showed no ATP hydrolysis on its own (data not shown). The values from the 1:2 dilution showed a stimulation by GST-Tma23(FL) and both truncations. In contrast, the values from the 1:5 dilution revealed no significant stimulation of the ATPase activity, no matter which Tma23 variant was added. Interestingly, there was the tendency that addition of total yeast RNA did not further increase the stimulation of the co-factors. This might result from the RNase A treatment during GST-purification. It cannot be excluded that some RNase was still present, since no SEC had been performed after the protein purification. The value from the 1:2 dilution would confirm this assumption, because addition of RNA alone stimulated the ATP hydrolysis of FLAG-Prp43. In contrast, the 1:5 dilution showed even a repression of FLAG-Prp43 activity when only RNA was added. To be sure whether there was a problem with the RNA preparation or the remaining RNase within the GST-eluates led to this result, one has to repeat the experiment.

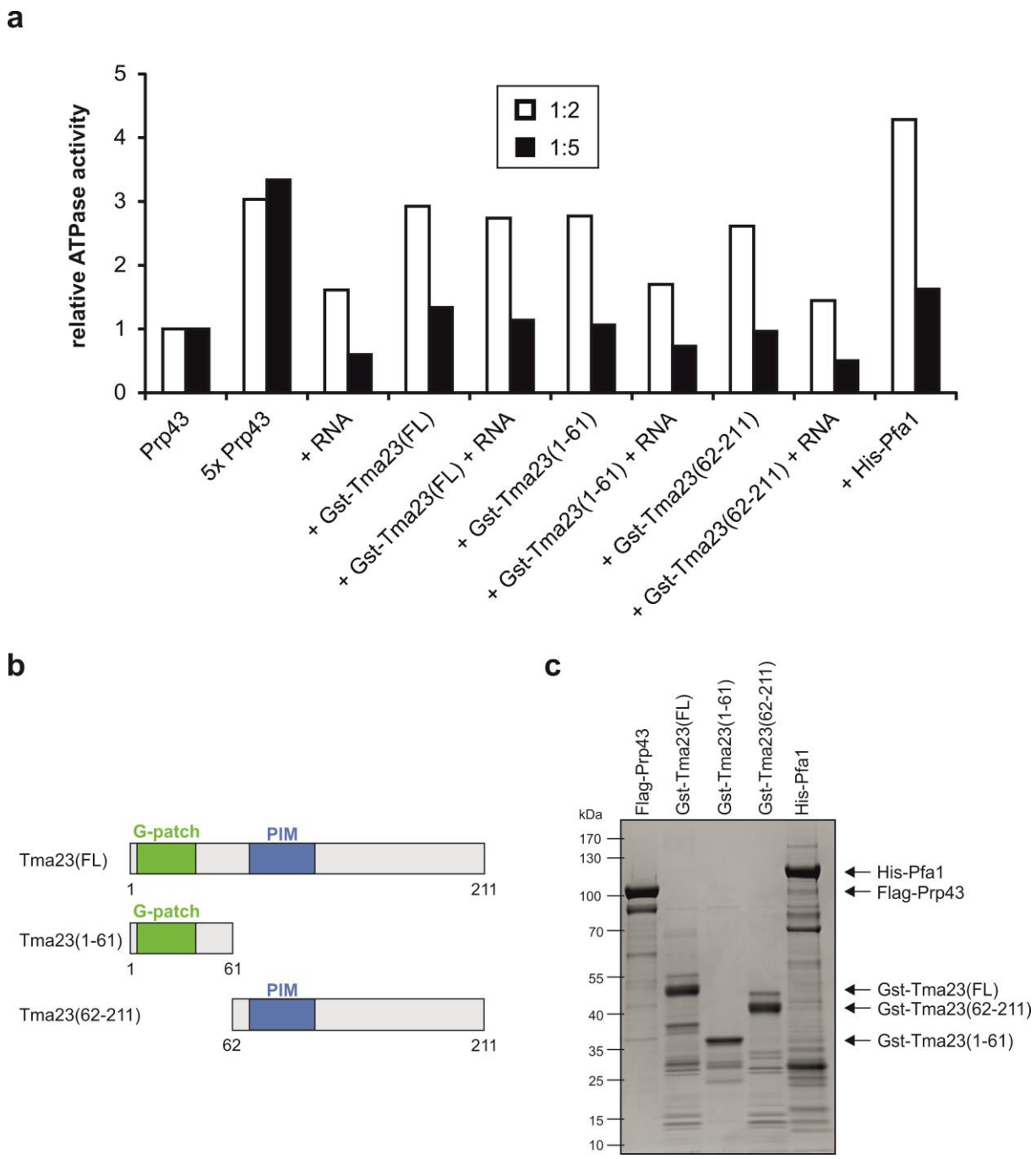

Figure 12: Analysis of the ATPase activity of FLAG-Prp43 in presence or absence of GST-Tma23(FL) and truncated versions. (a) The relative ATPase activity of FLAG-Prp43 [100 nM] in presence or absence of the indicated co-factors [~500 nM] was determined using the Malachite Green Phosphate Assay. When it is indicated, total yeast RNA (W303) was added. The assay was performed in a buffer containing 25 mM Tris/HCl pH 7.5, 150 mM NaCl, 10 mM $MgCl_2$ and 0.2 mM DTT. GST-tagged proteins were purified via GST-purification, FLAG-Prp43 was purified using the FLAG-purification protocol and His-Pfa1 was purified via His-purification. After incubation for 30 minutes at 37°C for ATP hydrolysis the mixtures were diluted (1:2 and 1:5). Dilutions were mixed with the working reagent and incubation for 30 minutes followed. Subsequently, the absorbance at an OD of 600 nm was measured in duplicates. **(b)** Schematic depiction of the Tma23 variants used for the ATPase assay displayed in (a). **(c)** Protein eluates that were used for the ATPase assay depicted in (a) were analyzed using SDS-PAGE followed by Coomassie blue staining. To check the protein amount used for one ATPase reaction with a total volume of 100 µl the same volume of each protein preparation that was used for one reaction was loaded.

The analysis of the protein eluates via SDS-PAGE and Coomassie staining implied that the molecular excess of the co-factors over the helicase, in the ATPase assay was presumably less than fivefold. Hence, the amount of the co-factors may have been too low to stimulate the ATPase activity of Prp43 sufficiently to be detected in this assay. In case of doubt one should probably add more protein, since both Coomassie blue staining and Bradford determination are not completely quantitative methods.

In summary, we can conclude that there is a hint that GST-Tma23 stimulates the ATPase activity of FLAG-Prp43. However, further optimization with respect to yield and purity of proteins and negative control is necessary to obtain clear results.

3.3 Tma23 shows a genetic interaction with the G-patch protein Pxr1

To investigate whether there is a functional link between Pfa1, Pxr1 and Tma23 we examined their genetic interaction. The growth behavior of the single knock out, each combination of double knock out and the triple knock out strain was tested in a dot spot assay.

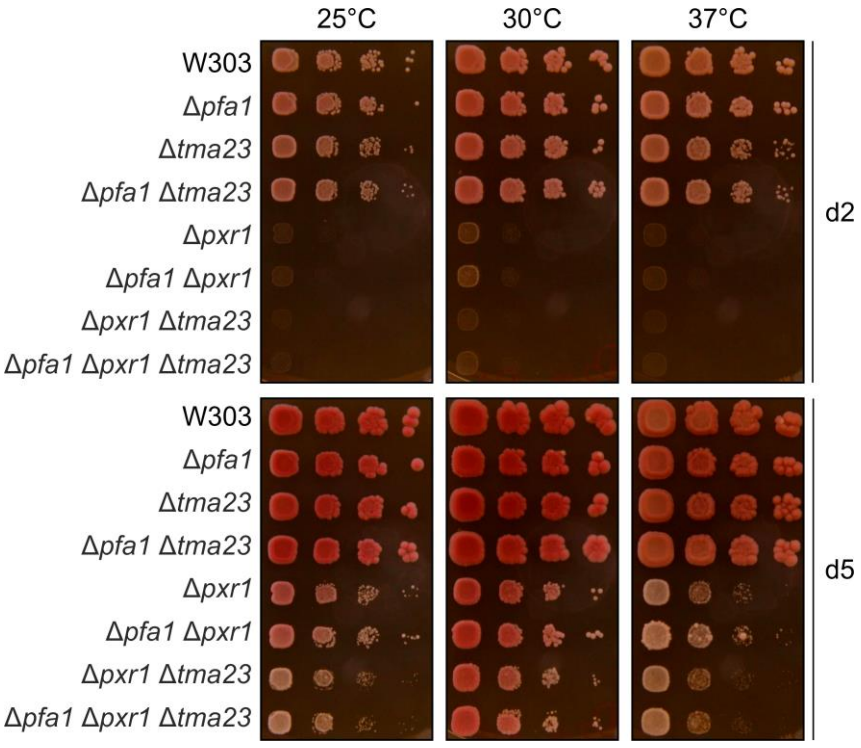

Figure 13: Genetic interaction between the G-patch proteins *PFA1*, *PXR1* and *TMA23.* Wildtype (W303), single knock out (Δ*pfa1*, Δ*pxr1*, Δ*tma23*), each combination of double knock out (Δ*pfa1*Δ*tma23*, Δ*pfa1*Δ*pxr1*, Δ*pxr1*Δ*tma23*) and the triple knock out (Δ*pfa1*Δ*pxr1*Δ*tma23*) strains were spotted in serial 10-fold dilution steps onto YPD plates to test the growth behavior at 25°C, 30°C and 37°C. Pictures were taken after incubation for two (d2) and five (d5) days.

As expected, deletion of *PFA1* had no noticeable impact on growth (figure 13, d2), while the lack of *PXR1* led to a severe growth defect (figure 13 d2, d5). The Δ*tma23* strain showed also impairment in growth, but not as drastic as the Δ*pxr1* strain (figure 13, d2). When *PFA1* deletion was combined with Δ*tma23* no enhancement of the Δ*tma23* phenotype could be observed (figure 13, d2). Interestingly, additional deletion of *PFA1* in the Δ*pxr1* strain reduced the growth defect due to Δ*pxr1,* while Δ*tma23* combined with Δ*pxr1* enhanced the phenotype (figure 13, d5). No further enhancement was observed when *PFA1* deletion was combined with the double knock out of *PXR1* and *TMA23* (figure 13, d5). Incubation at different temperatures had no impact on genetic interactions. These findings imply a genetic interaction between *PXR1* and *TMA23*, but not between *PFA1* and *TMA23*.

3.4 The unknown factor Gaf1 (Ycr016w) directly interacts with Prp43

An up to now unknown ribosome biogenesis factor, Ycr016w, was shown to be associated to three G-patch proteins of Prp43 (Pfa1, Pxr1 and Cmg1) and to co-purify Prp43 in TAP (Stefan Unterweger, in progress). Since the protein sequence of Ycr016w does not reveal a glycine-rich motif it cannot be assigned to G-patch proteins. However, there is a link between this unknown factor and the G-patch proteins of Prp43 and we therefore named the protein *G-patch protein associated factor 1* (Gaf1). We suspected that this protein might act as adapter protein of Prp43 like it is known for Ntr2 that is involved in the recruitment of Prp43 to the lariat-spliceosome complex during mRNA splicing (Tanaka et al., 2007; Tsai et al., 2005).

Hence, we aimed to examine the direct interaction between Gaf1 and Prp43 and performed an *in vitro* interaction assay. Therefore, His-Gaf1 and FLAG-Prp43 were co-expressed in *E. coli* BL21, thereby allowing the complex to form already in the course of the protein synthesis. We performed a FLAG-purification of Prp43, followed by a His-purification of Gaf1. If the two proteins form a complex, both proteins should be recovered after the two-step purification (figure 14). As a negative control both proteins were expressed separately in *E. coli* BL21 and were subjected to the same purification protocol outlined before. None of the separately expressed proteins should occur in the eluate after the second purification step (figure 14a).

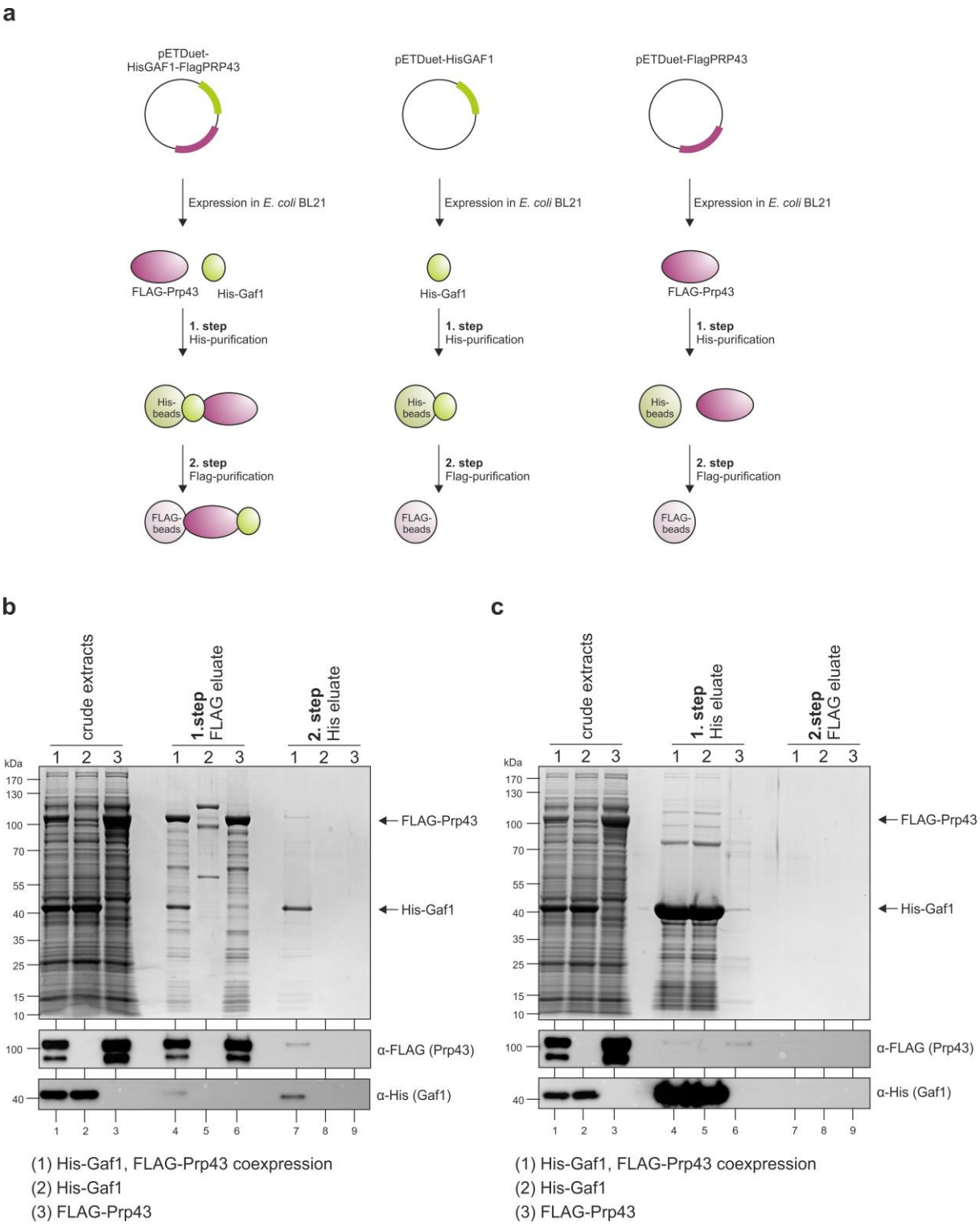

Figure 14: Gaf1 forms a stable complex with the RNA helicase Prp43. (a) Experimental scheme of the *in vitro* interaction assay to examine the ability of Gaf1 to bind Prp43. His-Gaf1 and FLAG-Prp43 were co-expressed in *E. coli* BL21 and were purified via a two-step purification. First, a FLAG-purification of Prp43 was performed, followed by a His-purification of Gaf1. As a negative control both proteins were expressed separately and subjected to the same purification protocol. The FLAG- and the His-eluate were analyzed using SDS-PAGE and Coomassie staining as well as western blotting using α-His and α-FLAG antibodies. The recovery of both proteins after the two-step purification indicates a direct interaction between Gaf1 and Prp43. **(b)** His-Gaf1 directly

interacts with FLAG-Prp43 *in vitro*. The Prp43 binding ability of Gaf1 was investigated using the experimental procedure outlined in (a). **(c)** Inverse experiment to the in vitro interaction assay outlined in (a). To confirm the results in (b) the inverse experiment was carried out performing a His-purification of Gaf1 followed by a FLAG-purification of Prp43.

Coomassie staining and western blot analysis revealed that Gaf1 and Prp43 form a complex, since both proteins occurred in the FLAG- as well as in the His-eluate (figure 14b, lanes 4 and 7). Unspecific binding of His-Gaf1 to the FLAG- and FLAG-Prp43 to the His-beads can be ruled out, because there was no His-Gaf1 in the FLAG- (figure 14b, lane 5) and no FLAG-Prp43 in the His-eluate (figure 14b, lane 9). Unexpectedly, FLAG-Prp43 from the FLAG-eluate (figure 14b, lane 4) could not be completely recovered in the His-eluate. This finding indicates a weak interaction between these two proteins, since the complex disassembled during the second purification step.

Additionally, there was a problem with the western blotting, since the ratio of His-Gaf1 in the western blot was altered compared to the Coomassie gel.

To confirm these observations we performed the inverse experiment using His-purification in the first step to purify Gaf1 followed by the second purification step using FLAG-beads to purify Prp43. Again, only in case of a direct interaction between Gaf1 and Prp43 both proteins should appear in the FLAG-, the second eluate. Although both proteins could be observed in the His-eluate after the first purification step, there was no stoichiometric complex as in the *in vitro* interaction assay before (figure 14c, lane 4). Only small amounts of FLAG-Prp43 in contrast to His-Gaf1 could be recovered. Hence, it is not surprising that the second eluate, after FLAG-purification, contained none of the two proteins, since the amount of FLAG-Prp43 was too low for another purification step. Considering the result from the inverse assay before, where the FLAG-purification (first step) revealed a stoichiometric complex of FLAG-Prp43 and His-Gaf1 (figure 14c, lane 4), but FLAG-Prp43 could not be recovered after the His-purification (second step) (figure 14c, lane 7), we supposed that there is a steric hindrance of complex formation when using His-beads for the purification. However, we have identified Gaf1 as a novel co-factor of Prp43 that specifically interacts with the helicase.

4 Discussion

In the yeast *S. cerevisiae* two G-patch proteins were demonstrated to interact with the DEAH/RHA helicase Prp43 in ribosome biogenesis (Chen et al., 2014; Lebaron et al., 2009; Pertschy et al., 2009). While Pfa1 together with Prp43 plays an important role in the last processing step of 18S rRNA maturation (Lebaron et al., 2009; Pertschy et al., 2009), Pxr1 is required for Prp43 function in 35S rRNA processing (Chen et al., 2014). As it was shown for other G-patch proteins (Christian et al., 2014; Heininger et al., 2016; Silverman et al., 2004), Pfa1 and Pxr1 functions rely on the G-patch domain. Direct interaction with Prp43 as well as the stimulation of its ATPase and helicase activity is mediated by this glycine-rich motif (Chen et al., 2014; Lebaron et al., 2009).

We have identified another G-patch containing protein that was shown to be linked to Prp43 and ribosome biogenesis (Kressler D., Unterweger S., in progress). Our *in vitro* interaction assays revealed a direct interaction between Tma23 and Prp43 (figures 8b and 8d) and corroborated results from yeast-two-hybrid (Y2H) studies performed by our cooperation partner Dieter Kressler (Kressler D., unpublished). Tma23 interacted with Prp43 via a domain downstream of the G-patch, which confirmed results from the Y2H experiments that revealed a minimal interaction fragment between amino acids 71 and 110 that contains the Prp43 interaction motif (PIM), which was also found in the previously identified primary Prp43 binding site of Pxr1 (Banerjee et al., 2015), but not in other Prp43 G-patch proteins (Kressler D., not published). Our findings indicated that the G-patch domain of Tma23 does not stably bind to Prp43 (figure 8b lane 7), even though Prp43 was found to weakly bind to GST-Tma23(1-61) (figure 8d, lane 7). As discussed above (section 3.1), the loading of the bait proteins in this assay was not equalized which is why FLAG-Prp43 is overrepresented in the eluate of GST-Tma23(1-61). Hence, we conclude that there is no stable interaction between the G-patch of Tma23 and Prp43, which is in contrast to other G-patch proteins (Chen et al., 2014; Heininger et al., 2016; Lebaron et al., 2009; Tanaka et al., 2007). However, a transient interaction between the Tma23 G-patch and the helicase likely occurs, if Tma23 really stimulates the activities of Prp43 via its G-patch. In the pretest of our ATPase assays GST-Tma23 stimulated the ATPase activity of FLAG-Prp43, however we could not show that the observed stimulation is Tma23 specific. Our results emphasized the need of further protein purification via SEC. Remaing RNase A from the GST-purification and remaining *E. coli* contaminants have to be removed. Therefore, more than 4 liters of *E. coli* culture is needed to gain a good protein yield after SEC, since GST-Tma23(FL) and GST-Tma23(62-211) purifications did not provide sufficient amounts of protein. Furthermore, we suppose that the

insufficient protein yield of GST-Tma23(FL) and Tma23(62-211) results from the strongly positively charged C-terminal part of Tma23, since the N-terminal part can be purified in great amounts. Hence, we plan to construct and express another truncation that comprises the G-patch as well as the Prp43 interaction surface but lacks the very positively charged C-terminal part. If the purification of this variant provides sufficient protein for the ATPase assays we can use this truncation instead of the full-length Tma23 for the ATPase assays. Furthermore, helicase assays are planned (by Blaud M.) to check whether Tma23 is also capable to stimulate the helicase activity of Prp43. These experiments are crucial to show whether Tma23 functions as activator of Prp43.

The investigation of the genetic network between *TMA23* and the two known G-patch proteins *PFA1* and *PXR1* revealed that *TMA23* is genetically linked to *PXR1*, but not to *PFA1* (figure 13). It is known that deletion of *PXR1* causes an inhibition of 35S rRNA processing at sites A_0, A_1 and A_2, but that a proportion of 35S rRNA is normally processed (Guglielmi and Werner, 2002). Microarray experiments, however, demonstrated that lack of *TMA23* leads to a delayed cleavage at site A_2 within the 35S precursor rRNA (Peng et al., 2003). These facts indicate that the enhanced phenotype of cells lacking both *TMA23* and *PXR1* probably results from delayed A_2 cleavage of the proportion of 35S rRNA that would be normally processed in Δ*pxr1* cells. Another work links Tma23 to a different step in ribosome maturation. A mutant of Tma23 was shown to suppress the phenotype of the *nep1-1*^{ts} (Buchhaupt et al., 2007). Nep1 is a methyltransferase that catalyzes the second step during the unique hypermodification (m1acp3Ψ, 1-methyl-3-(3-amino-3-carboxypropyl)Ψ) at position 1191 within helix 35 of the 18S rRNA (Meyer et al., 2011). Probably, Tma23 is involved in the release of snR35 that is required for the first step of this hypermodification (Meyer et al., 2011) or is involved in structural RNA rearrangements in order to make modification sites accessible. Deletion of *PFA1* in Δ*tma23* cells had no further effect on growth (figure 13). This observation argues against the possibility that Tma23 represents the other putative G-patch protein that was suggested to take over the function of Pfa1 in Δ*pfa1* strains, which was speculated as reason for the absence of a growth phenotype in Δ*pfa1* strains (Lebaron et al., 2009). Interestingly, deletion of *PFA1* attenuated the severe growth defect in Δ*pxr1* cells (figure 13). This result can be explained by the sequestering of Prp43 to the cytoplasm by Pfa1 that was recently shown by overexpression of Pfa1 (Heininger et al., 2016). If Pfa1 is also absent, Prp43 can enter the nucleus and fulfill its functions in early steps of ribosome biogenesis. Deletion of *PFA1* in the Δ*pxr1*Δ*tma23* strain had neither a positive nor a negative impact on growth (figure 13) indicating that sequestering of Prp43 by Pfa1 has no additional effect on early steps of ribosome biogenesis when Tma23 and Pxr1

are absent. To prove these results deletions should be complemented to see whether each phenotype can be recovered by introducing the wildtype gene on a plasmid. Furthermore, another genetic interaction test will be done using a *pxr1*^{ts} mutant. Since the growth defect due to Δ*pxr1* is that drastic, one cannot exclude spontaneous mutations that lead to a suppression of the phenotype. Moreover, we suggest that it is easier to assess the effects of additional deletions in the *pxr1*^{ts} strain than in the knock out strain.

However, there are several lines of evidence that Pxr1 and Tma23 are functionally related. First, Tma23 and Pxr1 harbor a primary interaction domain that mediates the interaction with the helicase Prp43 (Banerjee et al., 2015) (figure 8) and contain a motif that is conserved in both proteins (Kressler D., not published). In contrast to other G-patch proteins that interact with the helicase via their G-patch domain (Heininger et al., 2016; Lebaron et al., 2009; Tanaka et al., 2007) the interaction of Prp43 with Pxr1 as well as with Tma23 appeared to be largely independent from the G-patch domain (Banerjee et al., 2015) (figure 8). Furthermore, both proteins are very small with a molecular weight of about 30 kDa compared to Pfa1 with a molecular weight of 87 kDa (see SGD, *Saccharomyces cerevisiae Genome Database*). Additionally, Tma23 as well as Pxr1 have a very high isoelectric point at about 11 which is in contrast to the very low isoelectric point of Pfa1 at about 6 (see SGD). The fact that deletion of *TMA23* causes a delayed A_2 cleavage (Peng et al., 2003) also indicates a link of Tma23 to early processing steps as it is known for Pxr1. Finally, our results demonstrated a genetic interaction between Pxr1, but not with Pfa1. However, a lot of further work has to be done to prove these speculations. Northern analysis and polysome profiles of Δ*tma23* strains would help to gain deeper insights into the function of Tma23 and whether it is indeed involved in early rRNA processing steps during ribosome biogenesis. Overexpression of Tma23 would be interesting to see whether Tma23 is capable to take over the function of Pxr1 in rRNA processing.

Beside the characterization of Tma23 this study revealed the identification of another co-factor of Prp43. Our *in vitro* interaction assay showed that Gaf1 directly binds Prp43. However, the purification via the His-beads seemed to be a problem, since the stoichiometric complex between FLAG-Prp43 and His-Gaf1 could not be recovered after His-purification. We suppose that there is a steric hindrance when using the His-beads for purification. That further indicates that the N-terminus of Gaf1 harbors the Prp43 interaction surface. Since the protein is N-terminally His-tagged, binding to the His-beads might displace FLAG-Prp43 from the N-terminal part of Gaf1. To prove these speculations one should perform another *in vitro* interaction assay using a C-terminally His-tagged Gaf1. If the interaction surface of Gaf1 is indeed located at the N-terminus, there should be no steric hindrance anymore and the

proteins should be recovered in a stoichiometric complex. Furthermore, truncated versions of Gaf1 should be tested for their binding ability to Prp43 to confirm the speculation about the localization of the Prp43 interaction surface of Gaf1. To investigate whether Gaf1 functions as Prp43 adapter protein in ribosome biogenesis, like it is known for Ntr2 in mRNA splicing (Tsai et al., 2005, 2007), one has to prove its impact on the recruitment of Prp43 to the precursor particles. Probably, Gaf1 also acts as partner of a G-patch protein to direct Prp43 to its sites of function, similar to the Ntr1-Ntr2 complex during mRNA splicing (Boon et al., 2006; Tanaka et al., 2007; Tsai et al., 2005, 2007). To address this, further binding studies with Prp43, Gaf1 and G-patch proteins should be done. Also Northern analysis and polysome profiles would help to understand the role of Gaf1 in ribosome biogenesis.

Our findings reveal the characterization of two unknown co-factors of Prp43 and indicate that the list of further Prp43 protein partners does not end. To understand the whole functional network between the helicase, its G-patch proteins and additional co-factors, like putative adapter proteins remain future challenges.

5 References

Aravind, L., and Koonin, E.V. (1999). G-patch: a new conserved domain in eukaryotic RNA-processing proteins and type D retroviral polyproteins. Trends Biochem. Sci. *24*, 342–344.

Arenas, J.E., and Abelson, J.N. (1997). Prp43: An RNA helicase-like factor involved in spliceosome disassembly. Proc. Natl. Acad. Sci. U. S. A. *94*, 11798–11802.

Banerjee, D., McDaniel, P.M., and Rymond, B.C. (2015). Limited Portability of G-Patch Domains in Regulators of the Prp43 RNA Helicase Required for Pre-mRNA Splicing and Ribosomal RNA Maturation in Saccharomyces cerevisiae. Genetics *200*, 135–147.

Bleichert, F., and Baserga, S.J. (2007). The Long Unwinding Road of RNA Helicases. Mol. Cell *27*, 339–352.

Bohnsack, M.T., Martin, R., Granneman, S., Ruprecht, M., Schleiff, E., and Tollervey, D. (2009). Prp43 Bound at Different Sites on the Pre-rRNA Performs Distinct Functions in Ribosome Synthesis. Mol. Cell *36*, 583–592.

Boon, K.-L., Auchynnikava, T., Edwalds-Gilbert, G., Barrass, J.D., Droop, A.P., Dez, C., and Beggs, J.D. (2006). Yeast Ntr1/Spp382 Mediates Prp43 Function in Postspliceosomes. Mol. Cell. Biol. *26*, 6016–6023.

Buchhaupt, M., Kötter, P., and Entian, K.-D. (2007). Mutations in the nucleolar proteins Tma23 and Nop6 suppress the malfunction of the Nep1 protein. FEMS Yeast Res. *7*, 771–781.

Chen, Y.-L., Capeyrou, R., Humbert, O., Mouffok, S., Kadri, Y.A., Lebaron, S., Henras, A.K., and Henry, Y. (2014). The telomerase inhibitor Gno1p/PINX1 activates the helicase Prp43p during ribosome biogenesis. Nucleic Acids Res. *42*, 7330–7345.

Christian, H., Hofele, R.V., Urlaub, H., and Ficner, R. (2014). Insights into the activation of the helicase Prp43 by biochemical studies and structural mass spectrometry. Nucleic Acids Res. *42*, 1162–1179.

Combs, D.J., Nagel, R.J., Ares, M., and Stevens, S.W. (2006). Prp43p Is a DEAH-Box Spliceosome Disassembly Factor Essential for Ribosome Biogenesis. Mol. Cell. Biol. *26*, 523–534.

Cruz, J. de la, Karbstein, K., Woolford, J.L., and Jr (2015). Functions of Ribosomal Proteins in Assembly of Eukaryotic Ribosomes In Vivo. Annu. Rev. Biochem. *84*, 93.

Fairman-Williams, M.E., Guenther, U.-P., and Jankowsky, E. (2010). SF1 and SF2 helicases: family matters. Curr. Opin. Struct. Biol. *20*, 313–324.

Fourmann, J.-B., Dybkov, O., Agafonov, D.E., Tauchert, M.J., Urlaub, H., Ficner, R., Fabrizio, P., and Lührmann, R. (2016). The target of the DEAH-box NTP triphosphatase Prp43 in Saccharomyces cerevisiae spliceosomes is the U2 snRNP-intron interaction. eLife *5*.

Fromont-Racine, M., Senger, B., Saveanu, C., and Fasiolo, F. (2003). Ribosome assembly in eukaryotes. Gene *313*, 17–42.

Guglielmi, B., and Werner, M. (2002). The Yeast Homolog of Human PinX1 Is Involved in rRNA and Small Nucleolar RNA Maturation, Not in Telomere Elongation Inhibition. J. Biol. Chem. *277*, 35712–35719.

Heininger, A.U., Hackert, P., Andreou, A.Z., Boon, K.-L., Memet, I., Prior, M., Clancy, A., Schmidt, B., Urlaub, H., Schleiff, E., et al. (2016). Protein cofactor competition regulates the action of a multifunctional RNA helicase in different pathways. RNA Biol. *13*, 320–330.

Henras, A.K., Soudet, J., Gérus, M., Lebaron, S., Caizergues-Ferrer, M., Mougin, A., and Henry, Y. (2008). The post-transcriptional steps of eukaryotic ribosome biogenesis. Cell. Mol. Life Sci. *65*, 2334–2359.

Henras, A.K., Plisson-Chastang, C., O'Donohue, M.-F., Chakraborty, A., and Gleizes, P.-E. (2015). An overview of pre-ribosomal RNA processing in eukaryotes. Wiley Interdiscip. Rev. RNA *6*, 225–242.

Huh, W.-K., Falvo, J.V., Gerke, L.C., Carroll, A.S., Howson, R.W., Weissman, J.S., and O'Shea, E.K. (2003). Global analysis of protein localization in budding yeast. Nature *425*, 686–691.

Jankowsky, E. (2011). RNA Helicases at work: binding and rearranging. Trends Biochem. Sci. *36*, 19–29.

Kressler, D., Hurt, E., and Baβler, J. (2010). Driving ribosome assembly. Biochim. Biophys. Acta BBA - Mol. Cell Res. *1803*, 673–683.

Lebaron, S., Froment, C., Fromont-Racine, M., Rain, J.-C., Monsarrat, B., Caizergues-Ferrer, M., and Henry, Y. (2005). The Splicing ATPase Prp43p Is a Component of Multiple Preribosomal Particles. Mol. Cell. Biol. *25*, 9269–9282.

Lebaron, S., Papin, C., Capeyrou, R., Chen, Y.-L., Froment, C., Monsarrat, B., Caizergues-Ferrer, M., Grigoriev, M., and Henry, Y. (2009). The ATPase and helicase activities of Prp43p are stimulated by the G-patch protein Pfa1p during yeast ribosome biogenesis. EMBO J. *28*, 3808–3819.

Leeds, N.B., Small, E.C., Hiley, S.L., Hughes, T.R., and Staley, J.P. (2006). The Splicing Factor Prp43p, a DEAH Box ATPase, Functions in Ribosome Biogenesis. Mol. Cell. Biol. *26*, 513–522.

Martin, A., Schneider, S., and Schwer, B. (2002). Prp43 Is an Essential RNA-dependent ATPase Required for Release of Lariat-Intron from the Spliceosome. J. Biol. Chem. *277*, 17743–17750.

Martin, R., Straub, A.U., Doebele, C., and Bohnsack, M.T. (2013). DExD/H-box RNA helicases in ribosome biogenesis. RNA Biol. *10*, 4–18.

Meyer, B., Wurm, J.P., Kotter, P., Leisegang, M.S., Schilling, V., Buchhaupt, M., Held, M., Bahr, U., Karas, M., Heckel, A., et al. (2011). The Bowen-Conradi syndrome protein Nep1 (Emg1) has a dual role in eukaryotic ribosome biogenesis, as an essential assembly factor and in the methylation of 1191 in yeast 18S rRNA. Nucleic Acids Res. *39*, 1526–1537.

Nickels, B.E., and Hochschild, A. (2004). Regulation of RNA Polymerase through the Secondary Channel. Cell *118*, 281–284.

Peng, W.T., Robinson, M.D., Mnaimneh, S., Krogan, N.J., Cagney, G., Morris, Q., Davierwala, A.P., Grigull, J., Yang, X., Zhang, W., et al. (2003). A panoramic view of yeast noncoding RNA processing. Cell *113*, 919–933.

Pertschy, B., Schneider, C., Gnädig, M., Schäfer, T., Tollervey, D., and Hurt, E. (2009). RNA Helicase Prp43 and Its Co-factor Pfa1 Promote 20 to 18 S rRNA Processing Catalyzed by the Endonuclease Nob1. J. Biol. Chem. *284*, 35079–35091.

Puig, O., Caspary, F., Rigaut, G., Rutz, B., Bouveret, E., Bragado-Nilsson, E., Wilm, M., and Séraphin, B. (2001). The Tandem Affinity Purification (TAP) Method: A General Procedure of Protein Complex Purification. Methods *24*, 218–229.

Robert-Paganin, J., R&#xe9, Ty, S., phane, Leulliot, N., Robert-Paganin, J., R&#xe9, Ty, S., phane, and Leulliot, N. (2015). Regulation of DEAH/RHA Helicases by G-Patch Proteins, Regulation of DEAH/RHA Helicases by G-Patch Proteins. BioMed Res. Int. BioMed Res. Int. *2015*, *2015*, e931857.

Silverman, E.J., Maeda, A., Wei, J., Smith, P., Beggs, J.D., and Lin, R.-J. (2004). Interaction between a G-patch protein and a spliceosomal DEXD/H-box ATPase that is critical for splicing. Mol. Cell. Biol. *24*, 10101–10110.

Tanaka, N., Aronova, A., and Schwer, B. (2007). Ntr1 activates the Prp43 helicase to trigger release of lariat-intron from the spliceosome. Genes Dev. *21*, 2312–2325.

Thomson, E., Ferreira-Cerca, S., and Hurt, E. (2013). Eukaryotic ribosome biogenesis at a glance. J. Cell Sci. *126*, 4815–4821.

Tsai, R.-T., Fu, R.-H., Yeh, F.-L., Tseng, C.-K., Lin, Y.-C., Huang, Y., and Cheng, S.-C. (2005). Spliceosome disassembly catalyzed by Prp43 and its associated components Ntr1 and Ntr2. Genes Dev. *19*, 2991–3003.

Tsai, R.-T., Tseng, C.-K., Lee, P.-J., Chen, H.-C., Fu, R.-H., Chang, K., Yeh, F.-L., and Cheng, S.-C. (2007). Dynamic interactions of Ntr1-Ntr2 with Prp43 and with U5 govern the recruitment of Prp43 to mediate spliceosome disassembly. Mol. Cell. Biol. *27*, 8027–8037.

Tschochner, H., and Hurt, E. (2003). Pre-ribosomes on the road from the nucleolus to the cytoplasm. Trends Cell Biol. *13*, 255–263.

Walbott, H., Mouffok, S., Capeyrou, R., Lebaron, S., Humbert, O., Tilbeurgh, H. van, Henry, Y., and Leulliot, N. (2010). Prp43p contains a processive helicase structural architecture with a specific regulatory domain. EMBO J. *29*, 2194–2204.

Warner, J.R. (1999). The economics of ribosome biosynthesis in yeast. Trends Biochem. Sci. *24*, 437–440.

Woolford, J.L., and Baserga, S.J. (2013). Ribosome Biogenesis in the Yeast Saccharomyces cerevisiae. Genetics *195*, 643–681.